CHALMERS
UNIVERSITY OF TECHNOLOGY

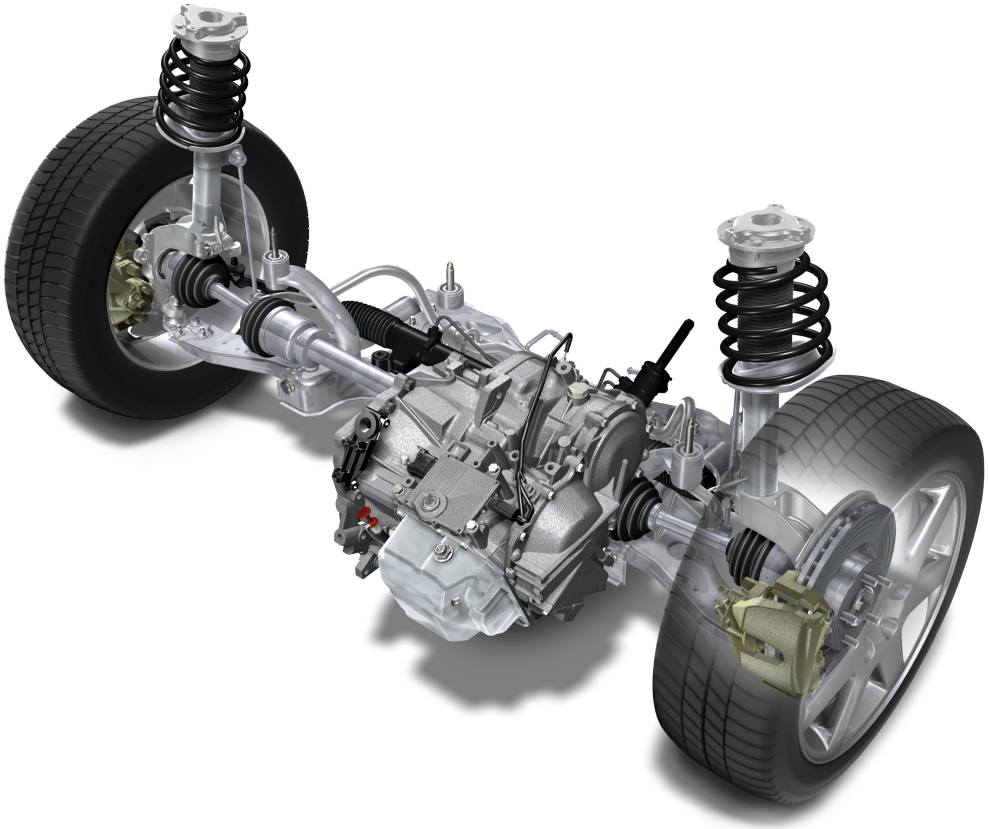

Objective Development of Damper Specification

Master's Thesis in Automotive Engineering

Ashrith Adisesh
Rohit Agarwal (KTH)

Department of Mechanics and Maritime Sciences
CHALMERS UNIVERSITY OF TECHNOLOGY
Gothenburg, Sweden 2018

Master's thesis 2018:28

A report on Objective Development of Damper Specification

Ashrith Adisesh
Rohit Agarwal (KTH)

CHALMERS
UNIVERSITY OF TECHNOLOGY

Department of Mechanics and Maritime Sciences
Division of Vehicle Engineering and Autonomous Systems
Vehicle Dynamics Group
Chalmers University of Technology
Gothenburg, Sweden 2018

Objective Development of Damper Specification
Ashrith Adisesh
Rohit Agarwal (KTH)

Supervisor: Mohit Asher, Volvo Car Corporation
Examiner: Matthijs Klomp, Department of Mechanics and Maritime Sciences

Master's Thesis 2018:28
Department of Mechanics and Maritime Sciences
Division of Vehicle Engineering and Autonomous Systems
Vehicle Dynamics Group
Chalmers University of Technology
SE-412 96 Gothenburg
Telephone +46 31 772 1000

Cover: Volvo S40/V50 Front Axle.

Typeset in LaTeX
Printed by Chalmers Reproservice
Gothenburg, Sweden 2018

DEGREE PROJECT IN VEHICLE ENGINEERING,
SECOND CYCLE, 30 CREDITS
STOCKHOLM, SWEDEN 2018

Objective Development of Damper Specifications

ROHIT AGARWAL

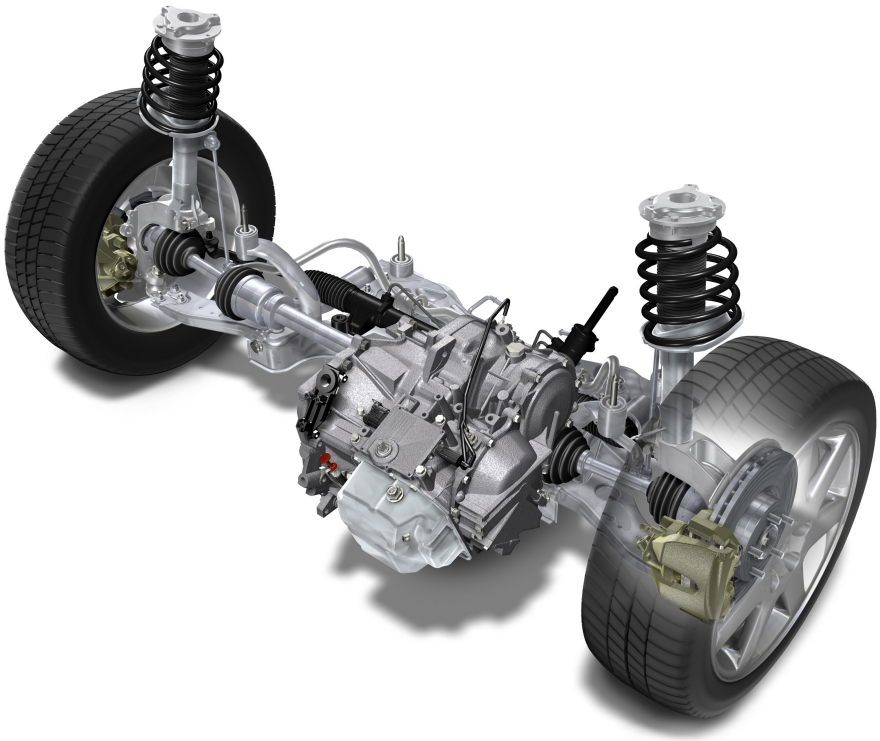

KTH ROYAL INSTITUTE OF TECHNOLOGY
SCHOOL OF ENGINEERING SCIENCES

TRITA -SCI-GRU 2018:412

Objective Development of Damper Specification
Rohit Agarwal
Ashrith Adisesh (Chalmers)

Supervisor: Mohit Asher, Volvo Car Corporation
Examiner: Lars Drugge, Department of Aeronautical and Vehicle Engineering

Master's ThesisTRITA-SCI-GRU 2018:412
Department of Aeronautical and Vehicle Engineering
KTH Royal Institute of Technology

Abstract

Damping of the sprung and un-sprung masses of a vehicle through a suspension damper is crucial to obtain good comfort and handling characteristics. Damper tuning, which is predominantly based on subjective feedback and experience from engineers takes up a large amount of time and resources. Preliminary knowledge of the influence of dampers in different operating regions can provide a good starting point in the damper tuning process. This research thesis aims to develop objective metrics related to the response of simplified vehicle models and could provide information regarding the modifications in the damper specifications to achieve the desired response.

Quarter-car models with linear, asymmetric and non-linear damper curves are simulated in the *Matlab* environment for step and swept sine inputs. The responses are further investigated to identify metrics of interest, by which the behaviour of the vehicle can be understood. For linear damper models, the poles of the system are analyzed and pole placement method is used to understand the behaviour of sprung and un-sprung masses when suspension parameters are varied. For asymmetric dampers, metrics which could help decide the required degree of asymmetricity between compression and rebound damping are presented. Finally, for non-linear dampers, the effect of damping force in different regions of operation is studied. A sensitivity analysis (Design of Experiments) is performed to identify the most influential variables corresponding to these metrics.

With these results, the response of the model is studied to obtain the metrics of interest which can be attributed to the behaviour of the vehicle. Comparisons are presented to visualize the effects of different damper specifications by which an initial prediction could be made for the damper specifications. This outcome can potentially enhance the preliminary knowledge of the effects of damper tuning and thereby providing a better starting point for the damper development process.

Keywords: System response, quarter-car, non-linear damper, objective metrics

Sammanfattning

Dämpning av fordonets fjädrade och ofjädrade massor genom en hjulupphängningsdämpare är avgörande för att uppnå god komfort och goda köregenskaper. Stötdämparinställningar baseras övervägande på subjektiv återkoppling och erfarenhet från ingenjörer vilket tar upp mycket tid och resurser. Preliminär kunskap om påverkan av stötdämparinställningar i olika driftområden kan ge en bra utgångspunkt i stötdämpartester. Detta examensarbete syftar till att utveckla objektiva mätvärden relaterade till svaret på förenklade fordonsmodeller och kan ge information om ändringar i stötdämparinställningarna för att uppnå önskat svar.

Kvartsbilsmodeller med linjära, asymmetriska och icke-linjära dämparkurvor simuleras i Matlab-miljön för steg och svepade sinusinsignaler. Svaren undersöks ytterligare för att identifiera mätvärden av intresse, genom vilket fordonets beteende kan förstås. För linjära dämparmodeller analyseras systemets poler och polplaceringsmetoden används för att förstå beteendet hos fjädrade och ofjädrade massor när upphängningsparametrar varieras. För asymmetriska dämpare presenteras mätvärden som kan hjälpa till att bestämma den erforderliga graden av asymmetricitet mellan kompressions och returdämpning. Slutligen studeras effekten av dämpningskraft i olika regioner av driftområden för icke-linjära dämpare. En känslighetsanalys (Design of Experiments) utförs för att identifiera de mest inflytelserika variablerna som påverkar dessa mätvärden.

Med dessa resultat studeras modellens svar för att erhålla de värden som kan hänföras till fordonets beteende. Jämförelser presenteras för att visualisera effekterna av olika dämparspecifikationer, genom vilka en första förutsägelse kunde göras för stötdämparspecifikationerna. Detta resultat kan potentiellt förbättra förståelsen för effekterna av olika dämparinställningar och därigenom ge en bättre utgångspunkt för stötdämparutvecklingsprocessen.

Nyckelord: Systemsvar, kvartsbil, icke-linjär dämpare, objektiva mätvärden

Acknowledgements

The thesis work was carried out at the Vehicle Dynamics CAE group at Volvo Car Corporation and the Department of Mechanics and the division of Vehicle Engineering and Automonous Systems at Chalmers University of Technology. I would first like to thank Rohit Agarwal, Master's student in Vehicle Engineering at KTH Royal Institute of Technology, with whom this thesis was performed with. I would like to thank Mohit Asher for supervising this thesis work and Jasiel Najera-Garcia for co-supervising and providing constant inputs and suggestions. Many thanks to my examiner Matthijs Klomp and the examiner from KTH, Lars Drugge, for their continued feedback through the thesis work. I extend my gratitude to Carl Sandberg, Manager of Vehicle Dynamics CAE for providing this opportunity to carry out the thesis and to the Vehicle Dynamics CAE group members at Volvo Cars for their assistance in the successful completion of this thesis.

Ashrith Adisesh, Gothenburg, June 2018

Rohit Agarwal, Gothenburg, June 2018

Organization

Thesis students:

1. Ashrith Adisesh, Chalmers University of Technology, adisesh@student.chalmers.se
2. Rohit Agarwal, KTH Royal Institute of Technology, ragarwal@kth.se

The research work was carried out at the Vehicle Dynamics CAE group at Volvo Car Corporation, Gothenburg.

	Name	**E-mail**
Academic Supervisor and Examiner at Chalmers	Matthijs Klomp	matthijs.klomp@chalmers.se matthijs.klomp@volvocars.com
Examiner at KTH	Lars Drugge	larsd@kth.se
Industrial Supervisors	Mohit Hemant Asher Jasiel Najera-Garcia	mohit.hemant.asher@volvocars.com jasiel.najera-garcia@volvocars.com

Abbreviations

CAE	-	Computer Aided Engineering
F-v	-	Force-velocity
DoF	-	Degree of Freedom
PSD	-	Power Spectral Density
LS	-	Slope of Low speed damping
HS	-	Slope of High speed damping
KP	-	Knee point
DoE	-	Design of experiment

Nomenclature

ω_s	-	Natural Frequency of sprung mass
ζ_{ref}	-	Damping of the reference system
ζ_{new}	-	Damping of the new system
c_{new}	-	Damping of the new system
c_{ref}	-	Damping of the reference system
m_{new}	-	Mass of the new system
m_{ref}	-	Damping of the reference system

Contents

List of Figures

List of Tables

1
Introduction

This master's thesis describes the development of objective metrics related to vehicle model response by which the effect of changing damper specifications can be understood to obtain a desired response of the system. This report explains the work process carried out to execute this thesis. A brief literature study and the theory involved in this thesis work is explained in Chapter 2. Chapter 3 describes the methodology undertaken to carry out the different tasks and the results obtained from this is explained in Chapter 4. Finally, the findings from the tasks carried out earlier are concluded in Chapter 5 and the scope for future work is explained in Chapter 6.

1.1 Background

One of the key factors to good vehicle response is good damping of the sprung and unsprung masses of the vehicle through a suspension system. The handling and comfort characteristics can be tuned to a large extent by tuning the damping characteristics, however conflicting requirements between the two limit the performance of the vehicle in the individual characteristics. Historically, many methods have been investigated to find the optimal balance between the two conflicting requirements, but there is a lack of in-depth objective metrics which can give insight about the conflicting requirements of sprung and unsprung masses, and thus there is limited knowledge of the vehicle response at early development phase. A significant amount of time and resources are spent during the testing phase to evaluate this subjectively and involves a lot of experience from test engineers.

1.2 Problem Statement

The hydraulic damper in the suspension of the vehicle is the main component contributing to the damping of the vehicle masses. The tuning of this component takes up a large portion of time and energy in the development of a vehicle suspension system. Damper tuning is predominantly based on subjective feedback from skilled engineers working with damper testing and vehicle testing. Preliminary knowledge of the influence of dampers in different operating regions can provide a good starting point in the damper tuning process when very little details of the vehicle is known. In an effort to reduce time and cost of development, using CAE tools, especially in the concept stage of the project could be beneficial.

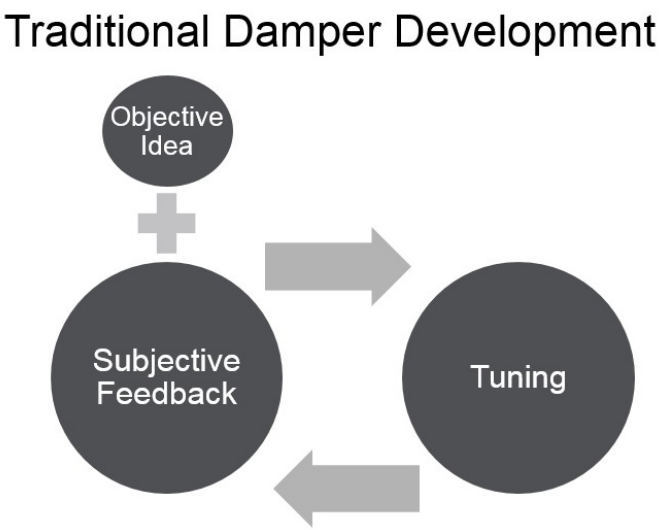

Figure 1.1: Traditional Damper Development Process

1.3 Objectives

The objective of this thesis is summarized in Figure 1.2. Traditional damper development, as shown in Figure 1.1 involves a lot of tuning and physical testing although there is a small amount of objective idea involved in it. With this thesis, the aim is to enhance this objective idea at the beginning of the vehicle development to provide a better starting point in the damper development process. This study aims to provide results by which comparisons can be presented to visualise the effects of different damper specifications by which an initial prediction could be made for the damper specifications. The idea here is to not eliminate the physical tests since that is a well proven method and there is belief that it will prevail for a long period of time, but to develop some additional knowledge to aid the engineers working with dampers at an early development phase and thus reduce some tuning phase time.

The thesis contains:

- An understanding of the conflicting requirements of sprung and unsprung masses with respect to damping force
- System response to different conditions of varying masses for different damping settings
- Analysis of quarter-car models for different damper curve (F-v curve)
- Sensitivity analysis (Design of Experiments) to understand the significance of the effects of different damper specifications on the sprung and unsprung mass responses
- Defining metrics of interest for the damper using the above knowledge
- Influence of identified metrics on the damper curve (F-v curve)

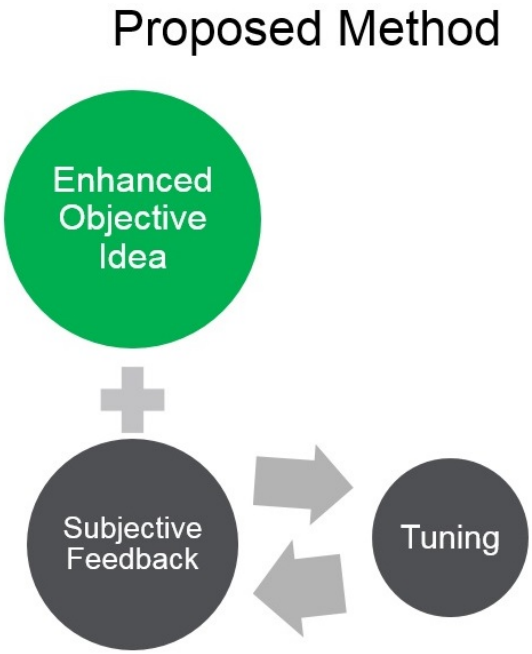

Figure 1.2: Proposed Damper Development Process

1.4 Research Questions

The outcome of this thesis intends to answer the following research questions.

- How does the unsprung mass respond if the sprung mass is varied and the same response is expected for the sprung mass?
- What is the nature of behaviour of the sprung mass and unsprung mass due to changes in damper specifications?
- With which aspects can the initial objective ideas of damper development be improved to minimise the "experience" factor and provide some objective insights?

1.5 Time Plan

A projected time plan with key milestones is shown Figure 1.3. Most of the tasks were followed according to plan although there were some deviations and modifications to the initially proposed time plan. The initial time plan can be found in the Planning Report attached in the Appendix.

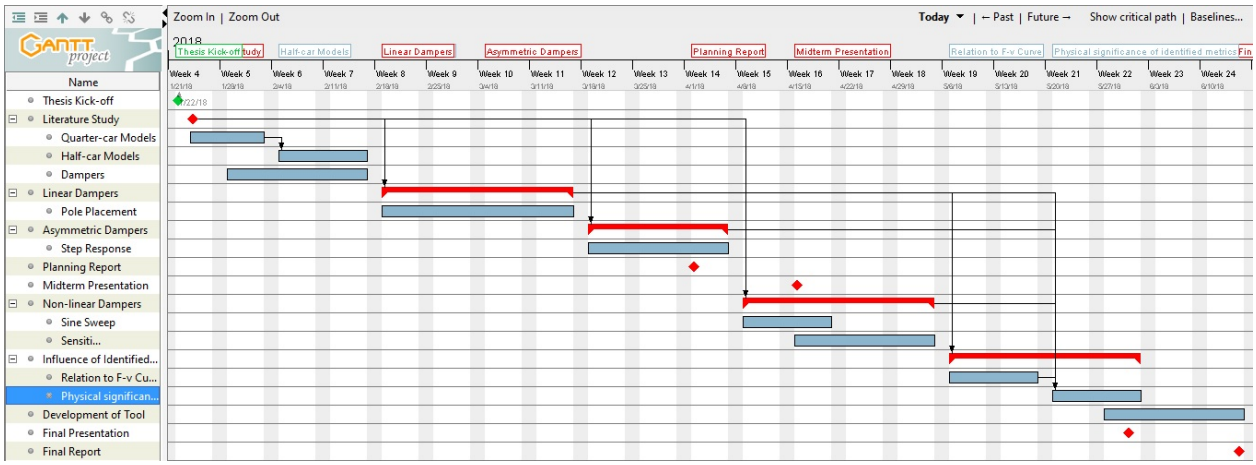

Figure 1.3: Time plan with key milestones

1.6 Limitations

Some simplifications and assumptions were considered in a few aspects for this thesis work.

- The construction and modeling of dampers is not considered, but the specifications of dampers are analysed.
- The damper curves are assumed to be piece-wise linear for the low speed and high speed regions.
- The vehicle parameters are not for any particular car but rather standard values are taken for the same.
- Compliance and tyre effects are neglected for quarter car model
- Friction forces are neglected in this study

2

Modeling and Analysis of Suspension Systems and Dampers

In this section, the theory related to the implementation of the work-flow is discussed. The theory is based on the literature study carried out in the particular topics. The chapter starts with some literature study related to research that has been done in this field to get some basic ideas. This is then followed by introduction to vehicle models and their analysis in frequency and s domain. After that an overview is given on the different kind of dampers which have been used further in this project.

2.1 Literature Study

The literature gives some idea about the influence of dampers and springs on ride and handing characteristic theoretically without providing in-depth analysis. In [1] and [2], discussions have been done regarding the conflicting requirements related to ride and handling and also the use of piston stroke dependent damper force along with velocity dependent force are discussed. Basics of damping and F-v curves have been discussed in [3] and [4] .

A lot of studies have also been done on optimisation of suspension parameters to reduce the transmissibility and acceleration of sprung mass system. The Frahm model [5] is one such system which focuses on reducing the transmissibilty of primary (sprung) mass system but does not focus on the ride hence the system get over damped. RMS optimisation of a cost function based on the transfer function of acceleration and sprung mass for the whole working frequency range of 0-20 Hz is presented in [6] and [7]. Design of experiment analysis has also been done in [8], which talks about the influence of spring, dampers and tyre pressure to ensure optimum ride comfort.

The study is next extended to asymmetric dampers.The need for asymmetric dampers has been briefly mentioned in [9]. An initial study on this has been carried out by [10], where the result of a shift in the mean position of the sprung mass caused by damping asymmetry is shown. The advantages of the asymmetric dampers over symmetric dampers for quarter-car and half-car models are shown in [11]. The find-

ings here show that asymmetric dampers produce smoother response for pitch/roll motion and also reduces the vertical acceleration level, which can be attributed to the comfort of passengers.

During the literature study, it was observed that most of the studies have been devoted towards finding different algorithms for optimisation of sprung mass displacement and acceleration to get a good compromise between ride and handling. However ride and handling is a subjective feeling which mostly depends on tuning. Also, most of the study focuses on the behaviour of sprung mass system when suspension parameters are changed, neglecting the effect on unsprung mass.

When it comes to understand the effect of dampers,which are velocity dependent, there is lack of literature which provides a thorough study of the influence of different damping regions on sprung and unsprung masses. Hence this study focuses on providing a picture about the behaviour of sprung and unsprung masses when suspension parameters are changed and also the effect of damping parameters in different velocity and frequency regions.

2.2 Quarter-car Model

Vehicles can generally be assumed to be a combined system of mass, spring and dampers. Based on the objective of analysis of vehicle suspension, the simplest model to start with is the quarter-car model.

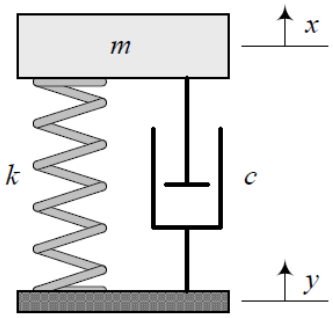

Figure 2.1: 1-DoF Quarter-car model [6]

The quarter-car represents the simplest form of a vehicle model with one corner of a car modelled as a mass, spring and damper system. Figure 2.1 is a representation of a one degree of freedom (1-DoF) linear quarter car model. One quarter of the mass of the car is modelled as a solid mass called sprung mass m, and is supported by the suspension with a linear spring of stiffness k and a linear damper with damping c. For a given input y, the equation of motion is given by equation 2.1

$$m\ddot{x} + c(\dot{x} - \dot{y}) + k(x - y) = 0 \tag{2.1}$$

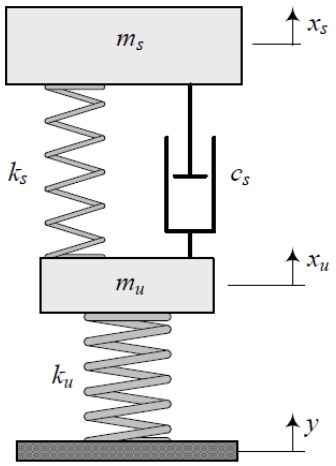

Figure 2.2: 2-DoF Quarter-car model [6]

The 1-DoF system considers the unsprung mass to be negligible, so only the sprung mass displacement (body bounce) is captured. Wheel-hop phenomenon which is dominant at higher frequency (around 10 Hz) is characteristic of the unsprung mass. So, a 2-DoF quarter-car is modelled by taking the unsprung mass into account. Figure 2.2 represents a 2-DoF quarter-car model consisting of two masses m_s and m_u which are the sprung mass and unsprung mass of the vehicle respectively. The sprung mass represents the mass of quarter of the car body and unsprung mass represents the mass of one wheel. The sprung mass is supported by a spring of stiffness k_s and damping c_s, which forms the main suspension. The stiffness of the tyre is modelled as a spring with stiffness k_u and the damping of the tyre (c_t) is considered to be negligible compared to the damping of the suspension. The displacements of the sprung mass and unsprung mass due to the excitation y are x_s and x_u respectively. The equations of motion of the 2-DoF system are given by equations 2.2 and 2.3.

$$m_s\ddot{x_s} + c_s(\dot{x_s} - \dot{x_u}) + k_s(x_s - x_u) = 0 \tag{2.2}$$

$$m_u\ddot{x_u} - c_s(\dot{x_s} - \dot{x_u}) - k_s(x_s - x_u) + k_u(x_u - y) = 0 \tag{2.3}$$

Equations 2.2 and 2.3 of the quarter-car model can be represented in a matrix form as $M\ddot{x} + C\dot{x} + Kx = F$, where

$$M = \begin{bmatrix} m_s & 0 \\ 0 & m_u \end{bmatrix}$$

$$C = \begin{bmatrix} c_s & -c_s \\ -c_s & c_s + c_t \end{bmatrix}$$

$$K = \begin{bmatrix} k_s & -k_s \\ -k_s & k_s + k_t \end{bmatrix}$$

$$F = \begin{bmatrix} 0 \\ k_t y + c_t \dot{y} \end{bmatrix}$$

The quarter-car model is the most simple representation of the vehicle suspension and forms the base of the analysis performed in this thesis.

2.3 Half-car Model

A half-car model considers one half of the vehicle with it's individual suspension for two wheels, either the front/rear or the left/right combinations. Half-car models are useful analyse modes of vibrations such as pitch and roll, which cannot be realized from a quarter-car model. A half-car model with two degrees of freedom for bounce and pitch/roll is the simplest form but from the perspective of this thesis, only the 4-DoF half-car model is explained.

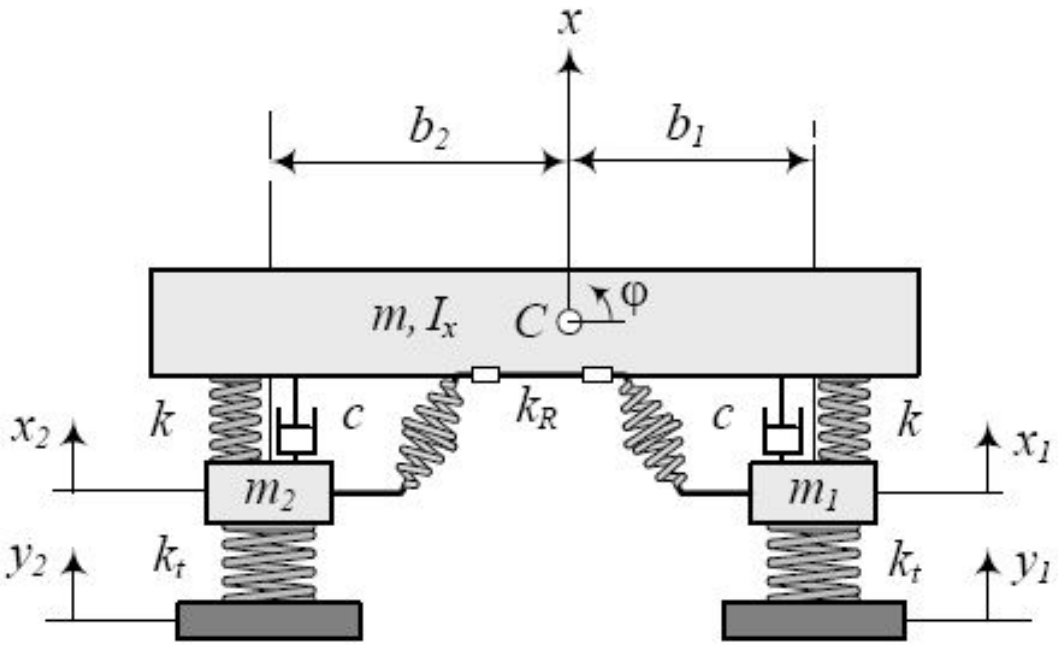

Figure 2.3: 4-DoF Half-car Bounce and Roll Model [6]

Figure 2.3 shows a 4-DoF half-car roll model with an anti-roll bar included. A symmetric suspension is assumed for the left and right wheels in this case. This model is helpful in analyzing the body roll motion along with the bounce motion and the unsprung mass motions. A reference to the parameters shown in Figure 2.3 is given in Table 2.1, and the equations of motion are given in equations 2.4 - 2.7

Table 2.1: Parameters of the 4-DoF half-car roll model

Parameter	Description
m	Sprung mass (Half of the total mass)
m_1	Left unsprung (tyre) mass
m_2	Right unsprung (tyre) mass
k	Suspension stiffness
c	Suspension damping
k_t	Tyre stiffness
k_R	Anti-roll bar stiffness
x	Sprung mass vertical displacement
x_1	Left unsprung mass vertical displacement
x_2	Right unsprung mass vertical displacement
ϕ	Body roll angle
I_x	Mass moment of inertia
y_1	Road excitation at left tyre
y_2	Road excitation at right tyre
b_1	Distance of CoG from left tyre
b_2	Distance of CoG from right tyre

$$m\ddot{x} + 2c\dot{x} + (cb_1 - cb_2)\dot{\phi} - c\dot{x_1} - c\dot{x_2} + 2kx + (kb_1 - kb_2)\phi - kx_1 - kx_2 = 0 \quad (2.4)$$

$$I_x\ddot{\phi} + (cb_1 - cb_2)\dot{x} + (cb_1{}^2 + cb_2{}^2)\dot{\phi} - cb_1\dot{x_1} + cb_2\dot{x_2} + (kb_1 - kb_2)x + (kb_1{}^2 + kb_2{}^2 + k_R)\phi - kb_1x_1 + kb_2x_2 = 0 \quad (2.5)$$

$$m_1\ddot{x_1} - c\dot{x} - cb_1\dot{\phi} + c\dot{x_1} - kx - kb_1\phi + (k + k_t)x_1 = y_1k_t \quad (2.6)$$

$$m_2\ddot{x_2} - c\dot{x} + cb_2\dot{\phi} + c\dot{x_2} - kx + kb_2\phi + (k + k_t)x_2 = y_2k_t \quad (2.7)$$

The equations 2.4-2.7 can also be written in a matrix differential form $M\ddot{X} + C\dot{X} + KX = FY$, similar to the 4-DoF half-car pitch model, which is convenient for simulations. The matrices X, M, C, K, F, Y for the 4-DoF roll model are given by

$$X = \begin{bmatrix} x \\ \phi \\ x_1 \\ x_2 \end{bmatrix} \quad (2.8)$$

$$M = \begin{bmatrix} m & 0 & 0 & 0 \\ 0 & I_x & 0 & 0 \\ 0 & 0 & m_1 & 0 \\ 0 & 0 & 0 & m_2 \end{bmatrix} \tag{2.9}$$

$$C = \begin{bmatrix} 2c & cb_1 - cb_2 & -c & -c \\ cb_1 - cb_2 & {cb_1}^2 + {cb_2}^2 & -cb_1 & cb_2 \\ -c & -cb_1 & c & 0 \\ -c & cb_2 & 0 & c \end{bmatrix} \tag{2.10}$$

$$K = \begin{bmatrix} 2k & kb_1 - kb_2 & -k & -k \\ kb_1 - kb_2 & {kb_1}^2 + {kb_2}^2 + k_R & -kb_1 & kb_2 \\ -k & -kb_1 & k + k_t & 0 \\ -k & kb_2 & 0 & k + k_t \end{bmatrix} \tag{2.11}$$

$$F = \begin{bmatrix} 0 & 0 & 0 & 0 \\ 0 & 0 & 0 & 0 \\ 0 & 0 & k_t & 0 \\ 0 & 0 & 0 & k_t \end{bmatrix} \tag{2.12}$$

$$Y = \begin{bmatrix} 0 \\ 0 \\ y_1 \\ y_2 \end{bmatrix} \tag{2.13}$$

2.4 Frequency Domain Analysis

The behaviour of vehicles at different frequencies is important as the different degrees of freedom have different resonance frequencies. Understanding the response at different frequencies will provide insight into the critical regions of interest from a damping point of view. The frequency response is studied by evaluating the transfer functions of three parameters in particular, which provides the amplitude ratio of input-to-output over the considered frequency range. The following parameters and their transfer functions were considered for evaluation [6].

- Transmissibility (Sprung mass displacement)
- Sprung mass acceleration
- Tyre force variation

Transmissibility and sprung mass acceleration are generally perceived as parameters which determine the comfort of the passengers and hence used for ride (primary) quality evaluation. The amount of road grip can be related to the variation of the amount of load on the tyres and this determines the handling quality of the vehicle. The expressions for the transfer functions corresponding to a 2-DoF quarter-car model excited with a single frequency are obtained from the equations of motion given in equations 2.2 - 2.3 expressed as matrices and then taking Fourier transforms of the obtained equations.

$$\begin{bmatrix} H_{x_r \to x_s} \\ H_{x_r \to x_u} \end{bmatrix} = (-\omega^2 M + i\omega C + K)^{-1}(i\omega C_t + K_t) \tag{2.14}$$

where, x_r is the road displacement, and M, C, K are matrices corresponding to the mass, damping and stiffness of both sprung and unsprung masses, and C_t, K_t are matrices corresponding to the damping and stiffness of the tyre respectively. The damping in the tyre C_t is considered to be negligible compared to the suspension damping and is thus neglected. ω is the angular frequency vector which determines the frequency range.

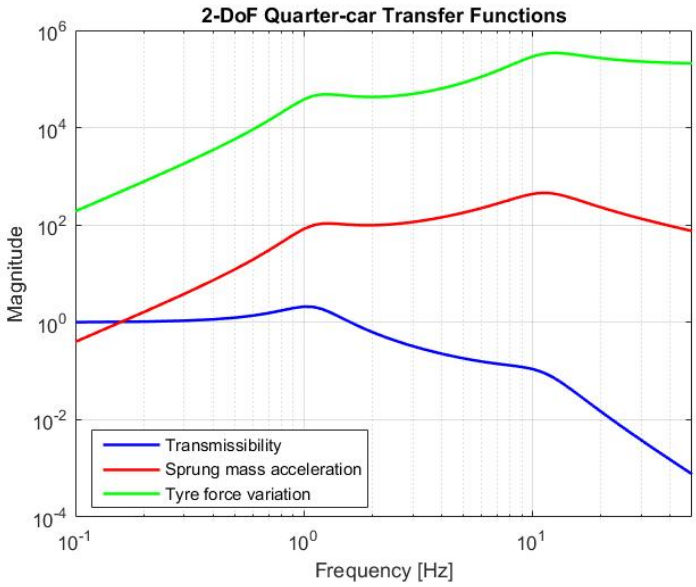

Figure 2.4: Transfer functions for a 2-DoF quarter-car model

$H_{x_r \to x_s}$ in equation 2.14 gives the transmissibility transfer functions and $H_{x_r \to x_u}$ gives the transfer function of the unsprung mass displacement. With these transfer functions computed, the transfer functions for sprung mass acceleration and tyre force variation can be calculated by

$$H_{x_r \to \ddot{x_s}} = -\omega^2 H_{x_r \to x_s} \tag{2.15}$$

$$H_{x_r \to \Delta F_{rz}} = k_t(1 - H_{x_r \to x_u}) \tag{2.16}$$

Figure 2.4 shows the transfer functions obtained from the equations 2.14, 2.15 and 2.16. These plots can be used to determine the magnitude of output for an input amplitude at a particular frequency. It can also be seen that there are two peaks in the transfer function plots around 1 Hz and 10 Hz, which correspond to the natural frequencies of the sprung mass and the unsprung mass respectively. The vibrations at these particular frequencies are also called bounce and wheel-hop modes. The larger the magnitude of x_s, $\ddot{x_s}$ and ΔF_{rz}, the worse is the parameter. Evaluation of ride-related parameters around the sprung mass natural frequency and evaluation of handling-related parameters at the unsprung mass natural frequency is of interest in this study.

2.5 Time Domain Analysis

2.5.1 Step Response

It is important to understand the system behaviour from a subjective point-of-view and the frequency analysis does not provide much information in this regard. Hence, there is a need to analyse the system in time domain as well. This analysis is based on a typical time varying input which generates a characteristic time response. Most of the available literature discusses about the optimisation of suspension parameters over a certain frequency range (0-20Hz) and not focus on the analysis of the behaviour of masses on different frequency sectors or single disturbances like step inputs. The time-domain analysis can then be extended into the laplace domain by investigating the poles of the system to understand the characteristics of the response. To start with, a step function is used as an input. The response is generated based on the transfer function $H(f)$ between the input and the displacement of sprung mass as output in laplace domain.

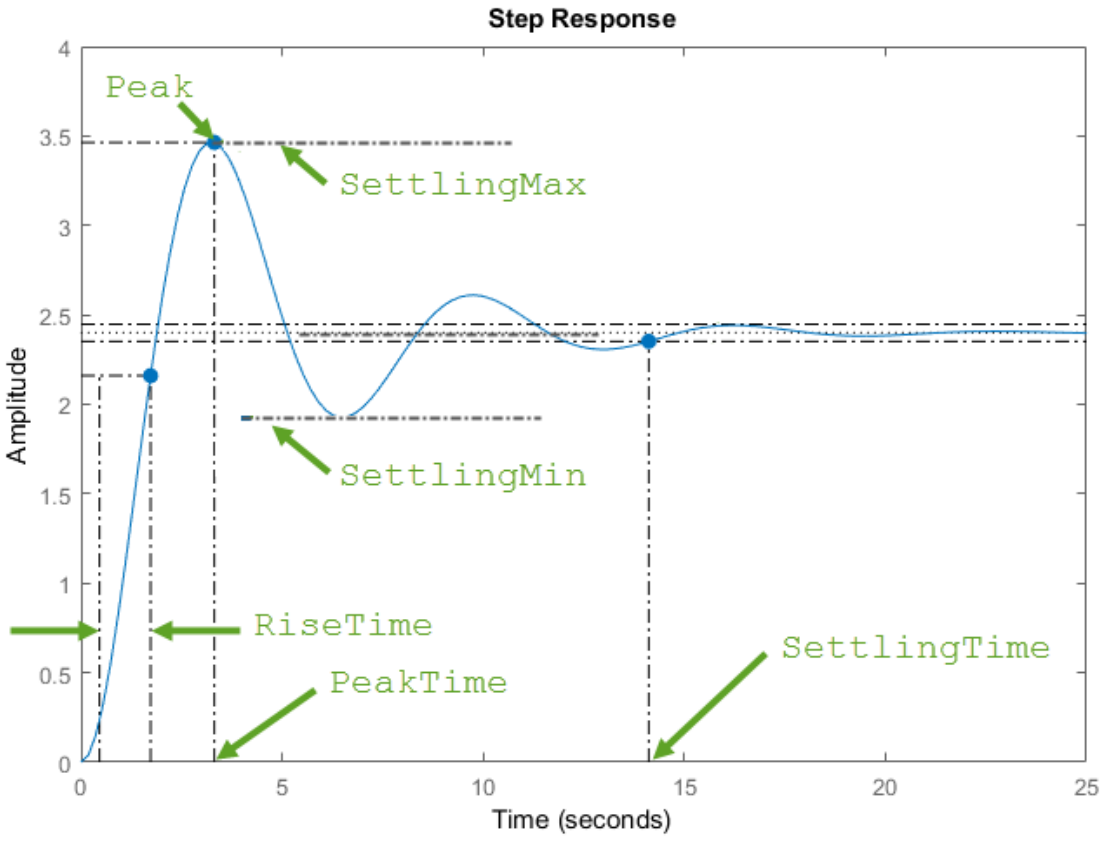

Figure 2.5: Characteristic step response [Ref: Mathworks]

From Figure 2.1, for a 1-DoF system,

$$H(f) = \frac{k}{ms^2 + cs + k} \tag{2.17}$$

Equation 2.18 can also be written in terms of natural frequency (ω_s) and damping ζ as

$$H(f) = \frac{\omega_s^2}{s^2 + 2\omega_s\zeta s + \omega_s^2} \tag{2.18}$$

Figure 2.5 shows the response of the transfer function in equation 2.18. This response could further be decomposed into simple terms to extract the information of a linear 1-DoF system. These terms are discussed below [12]:

- Rise time (T_r): Time taken for a response to go from 10% to 90% in amplitude. Analytic expression for rise time is hard to derive [12], but it is a function of ω_s and ζ.

- % Overshoot (OS): It refers the maximum value of the response with respect to the settling value.

$$\%OS = e^{-\frac{\zeta\pi}{\omega_n\sqrt{1-\zeta^2}}} \tag{2.19}$$

  From the equation, it can be observed that overshoot is just a function of damping (ζ) value.

- Peak Time (T_P): The time taken to reach the peak response value

$$T_P = \frac{\pi}{\omega_n\sqrt{1-\zeta^2}} \tag{2.20}$$

- Settling Time (T_s): The time required for the response to be within a certain percentage (2%) of the steady state value

$$T_s = \frac{4}{\omega_n\zeta} \tag{2.21}$$

2.5.2 Sine Sweep Response

The analysis is now extended to more real driving-like inputs rather than a simple step input. The sinusoidal input of reducing amplitude is swept over a certain frequency range. This input is considered since it replicates a real-life driving scenario on a standard road with high amplitude inputs at low frequencies and low amplitude inputs at higher frequencies. The range of swept frequencies is from 0.1 Hz to 20 Hz, since the intention here is to simulate the vertical dynamics of the vehicle. A sine sweep input signal is shown in Figure 2.6. A zoomed inset of the time history of the sine signal from 0 to 20 seconds is shown for better visualization of the increasing frequency and decreasing amplitude trend of the input signal.

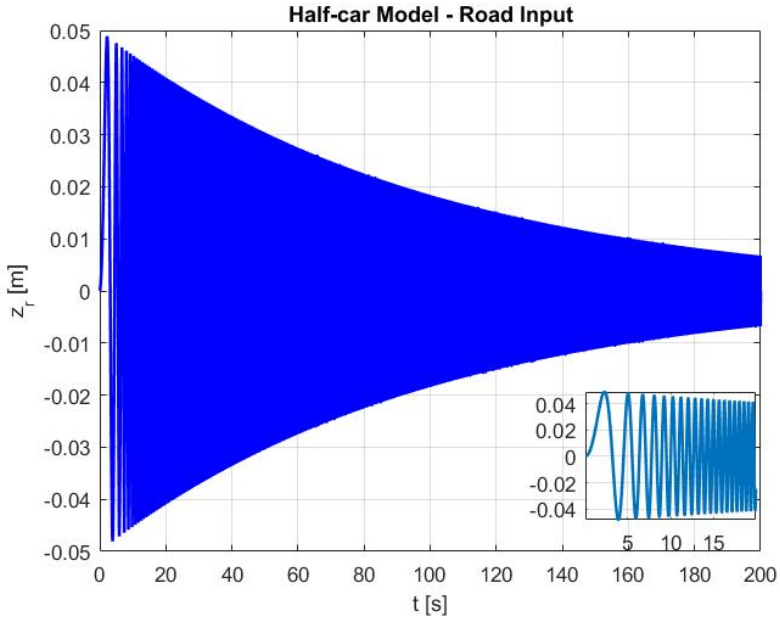

Figure 2.6: Sine Sweep Input Signal

An advantage of performing simulations for a sine sweep input is the fact that the frequency response of the system can also be studied. Analyzing the transfer functions in frequency domain is of importance to understand the vehicle behaviour at a particular frequency through Bode plots.

It also important to know the energy of the input signal and the Power Spectral Density (PSD) of the signal and this can be understood by the PSD plot shown in Figure 2.7.

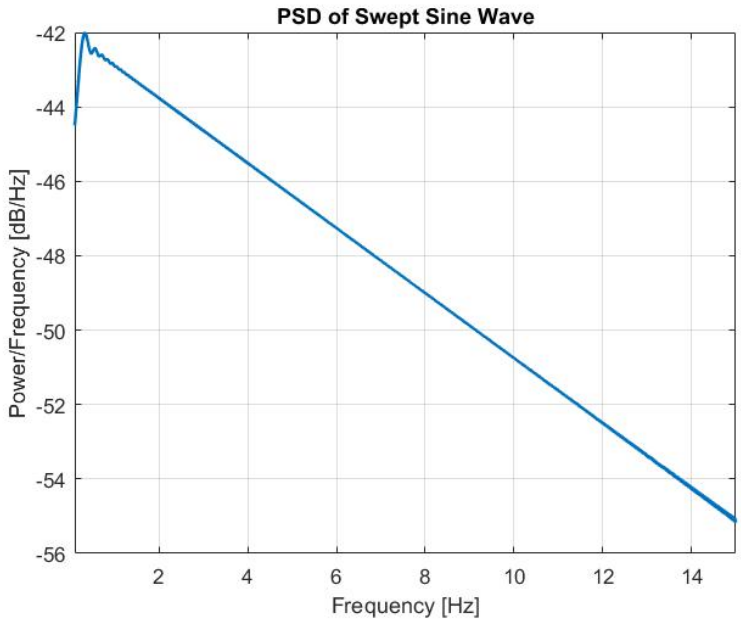

Figure 2.7: PSD of the swept sine wave

2.6 Poles Analysis

The metrics discussed in section 2.5 could also be determined using the poles of the system. Figure 2.8 depicts a pole-zero map in s-domain. The poles of the system is on the left side, which ensures that the system is stable. If the poles of a system are known, natural frequency (ω_n) is given by

$$\omega_n = \sqrt{x^2 + y^2} \tag{2.22}$$

Damping ratio ζ is given by

$$\zeta = cos(\theta) \tag{2.23}$$

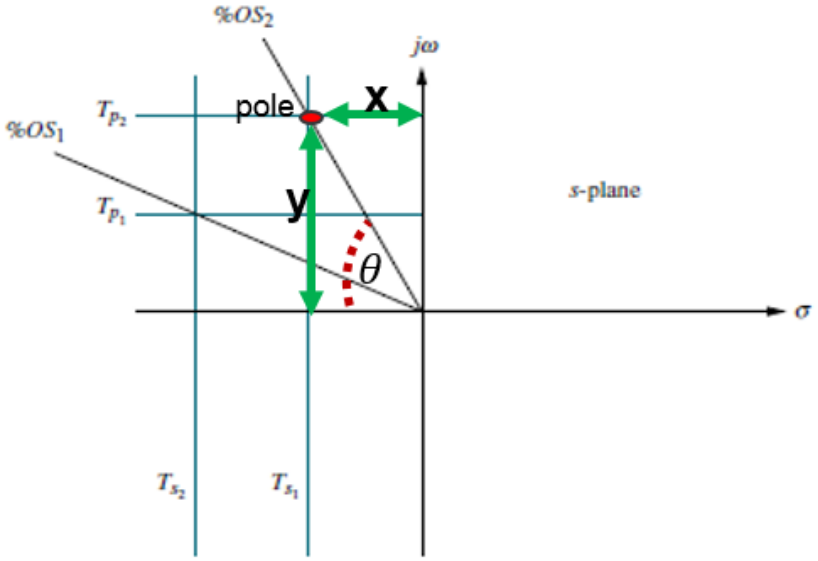

Figure 2.8: Poles in s-domain

Once, ω_s and ζ are known, the information regarding the system metrics discussed earlier can be generated. The pole analysis is useful while analyzing two different systems intended to provide the same output response which is explained in section 3.1.1. The shortcomings of the pole analysis is that it is valid only for a linear system and cannot be used when we move into non-linear dampers [12].

2.7 Dampers

Damping force is a function of the relative velocity between the sprung mass and the unsprung mass which in real world is non linear. A representation of the damper is the Force-velocity (F-v) curve which gives the relation between the velocity and the amount of damper force. The F-v curve for a damper is denoted in many different ways with different scaling parameters based on the requirement.

2.7.1 Linear Damper

A linear damper is the most simple form of representation of a damper. Figure 2.9 shows a typical F-v curve of a linear damper, where positive force indicates rebound forces and negative force indicates compression forces. It is also symmetric in compression and rebound, thus the damper force produced is a linear function of the damper velocity in both compression and rebound.

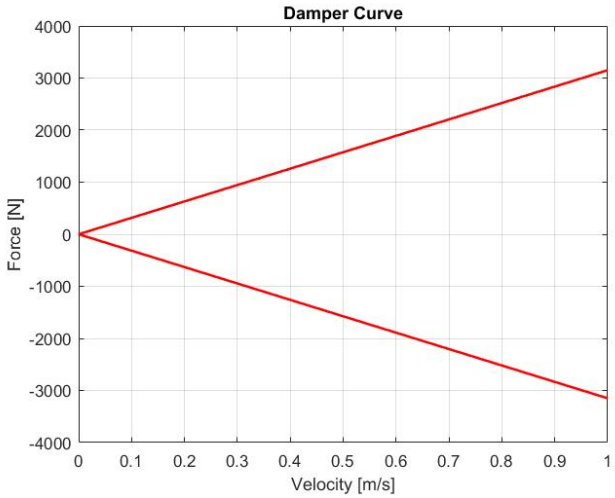

Figure 2.9: Linear symmetric damper curve

2.7.2 Asymmetric Damper

In practice, dampers are designed to produce higher forces during rebound and lower forces during compression. This is due to the fact that rebound controls the sprung mass movement and since the sprung mass is typically higher than the unsprung mass, the damping force required for rebound is higher. The same reasoning can be established for the lower compression force. Thus, the damper curve in reality is designed to be asymmetric in compression and rebound. This nature of damper curve is investigated for standard response inputs and it's effect is studied in the later chapters. It is important to note here that the damper curve is linear in rebound and compression and not to be mistaken for the non-linear damper in the following section. Figure 2.10 shows an asymmetric damper curve.

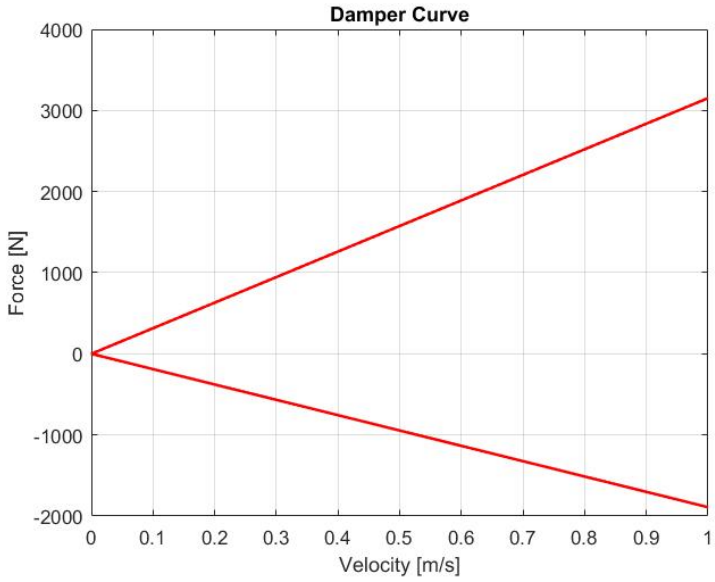

Figure 2.10: Linear asymmetric damper curve

2.7.3 Non-linear Symmetric Damper

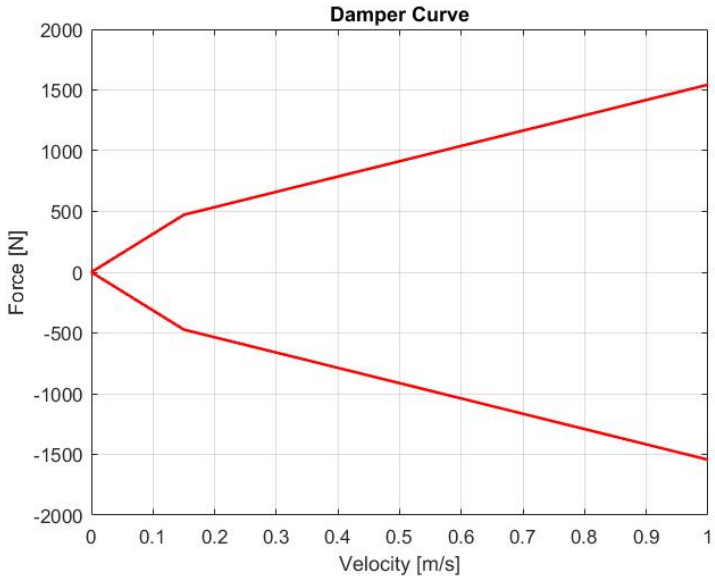

Figure 2.11: Non-linear symmetric damper curve

A F-v curve of a non-linear symmetric damper is shown in Figure 2.11. The compression forces are considered to be negative and the rebound forces to be positive and the rebound forces are usually higher than the compression forces but a symmetric compression and rebound force is shown in the figure for convenience. The damper curve is also classified into two regions, low speed and high speed based on the damper velocity. The point at which the split between the low and high speed region occurs is called the knee point. Higher damping forces at high damper

velocity can cause discomfort to passengers at high frequency/low amplitude. Thus, it is desired to have a lower damping for the high speed region compared to the low speed region. All these variables are important for this research study and are used for analysis by varying them individually. The effect of varying these damper variables and the reason for why should they be varied is studied in the following chapters

The design and modelling of dampers is rather complex and beyond the scope of this thesis, so only the effects of varying the variables is studied in an effort to establish objective numbers for the damper curve by which the effects of varying the damper curve variables on the different degrees of freedom can be captured to provide an insight into damper tuning. The analyses carried out in these topics are explained in the further chapters.

2.7.4 Non-linear Asymmetric Damper

This type of damper is a combination of the asymmetric damper (figure 2.10) and the non-linear damper (figure 2.11). A very brief analysis of the non-linear asymmetric damper is touched upon in this study.

3
Evaluation of Dampers

An overview of the methodology followed in this chapter in shown in Figure 3.1. The models were first simulated with linear dampers since it provides a simple and straight-forward starting point for the analysis. The analysis was then extended to simulations with asymmetric dampers to understand the variation in compression and rebound damping forces. The study was then carried out with non-linear dampers which is representative of dampers in reality.

The results from the above three damper analyses is used to identify metrics of interest for the different operating regions of the damper and finally provide some objective insight with the help of a tool.

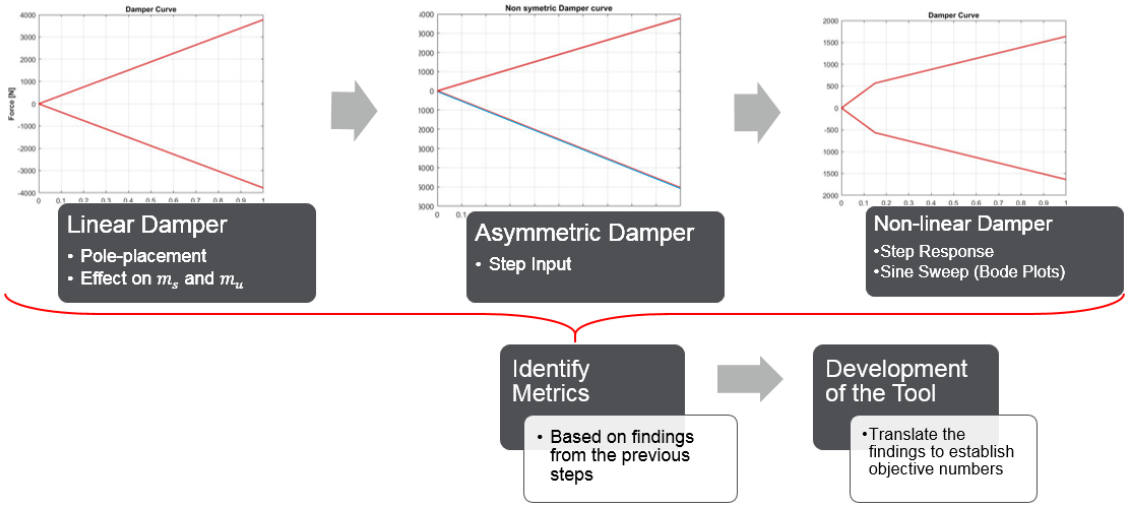

Figure 3.1: Work flow

3.1 Linear Damper

3.1.1 Matching Response

To start with, the first research question (Section 1.4) of understanding the unsprung mass response for having the same response of the sprung mass is studied. The idea here is to start with a reference system and then try to get the same response of the sprung mass with the new system with increased sprung mass and same natural frequency. The poles analysis discussed in Section 2.6 is applied in this study. A

1-DoF quarter car model with linear damper is considered. Table 3.1 shows the values of the parameters used for the reference 1-DoF system.

Table 3.1: Suspension parameters for reference 1DoF model

Parameter	**Value**
Sprung mass (m_s)	439.38 kg
Front suspension stiffness(k_s)	22589.2 N/m
Front suspension damping(c_s)	2113.62 Ns/m

Figure 3.2 shows the poles of this 1-DoF system, which can be found using equation 3.1. The poles are on the left side of the imaginary axis which ensures a stable system, and are conjugate to each other since it is an under-damped system.

$$s^2 + 2\omega_s\zeta_{ref}s + \omega_s^2 = 0 \tag{3.1}$$

For the new system with varied sprung mass, the natural frequency (ω_s) is desired to be the same as the reference system and thus a new spring stiffness value is obtained for this new system. The poles of the system could be found using equation 3.2.

$$s^2 + 2\omega_s\zeta_{new}s + \omega_s^2 = 0 \tag{3.2}$$

To have the same response, equation 3.1 and equation 3.2 should be equal to each other. Hence, comparing both the equations, it could be realized that,

$$\zeta_{ref} = \zeta_{new} \tag{3.3}$$

which on simplification gives,

$$c_{new} = c_{ref}\frac{m_{new}}{m_{ref}} \tag{3.4}$$

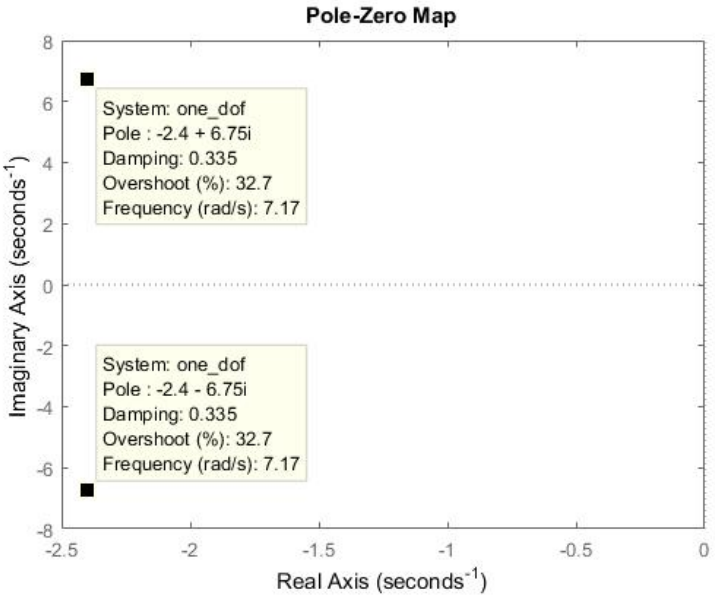

Figure 3.2: Poles of 1-DoF reference system

3.1.2 Pole Placement Method

The analysis with a 1-DoF model provides insight into the behaviour of the sprung mass but it is desired to understand the behaviour of the unsprung mass as well. To establish this understanding, a 2-DoF quarter-car model has to be considered. Since the characteristic equation of the 2-DoF system is a fourth order equation, it is tedious to formulate analytic expressions for the metrics discussed in the previous section. The next alternative is to carry out a comparative analysis, which still provides significant information regarding the desired outcome. The parameters of the 2-DoF system is shown in Table 3.2.

Table 3.2: Suspension parameters for reference 2-DoF model

Parameter	**Value**
Sprung mass (m_s)	439.38 kg
Front suspension stiffness(k_s)	22589.2 N/m
Front suspension damping(c_s)	2113.62 Ns/m
Unsprung mass(m_u)	42.27 kg
Tyre stiffness(k_t)	200000 N/m
Tyre damping(c_t)	352.27 Ns/m

Pole-placement technique is used for this analysis. Same methodology is followed for a 2-DoF system as well, where the idea is to match the response of the new system with a given reference system. A 2-DoF model has two sets of conjugate poles as shown in Figure 4.2a.

The poles which are closer to the origin are the dominant poles and they control the response of the sprung mass system. The effect of the other set of poles is negligible on the sprung mass since they are far away from the dominant poles. Also, when these poles are compared with the poles of 1-DoF system (with the same sprung mass), it is noticed that the dominant poles of the 2-DoF system are very close to the poles of the 1-DoF system in Figure 4.2b. Hence, by using equation 3.4, the response of sprung mass displacement could be matched approximately.

A variation is expected in the response of unsprung mass due to the fact that the effective force on unsprung mass system changes due to the change in stiffness and damping forces. To analyse the behaviour of the 2-DoF system, it is necessary to find the ζ and ω for the unsprung mass system. Equation 3.5 represents the general equation of poles for a 2-DoF system.

$$(s^2 + 2\omega_1\zeta_1 s + \omega_1^2)(s^2 + 2\omega_2\zeta_2 s + \omega_2^2) = 0 \tag{3.5}$$

Table 3.3: Parameters for 2-DoF model

Parameter	**Definition**
ω_1	Sprung mass frequency
ζ_1	Sprung mass damping ratio
ω_2	Unsprung mass frequency
ζ_2	Unsprung mass damping ratio

Table 3.3 gives the definition of all the parameters. The denominator of the transfer function of displacement for a 2-DoF system (Figure 2.2)is given by equation 3.6.

$$m_s m_u s^4 + [(m_s + m_u)c_s + m_s c_t]s^3 + [(m_s + m_u)k_s + m_s k_t + c_s c_t]s^2 + (c_s k_t + c_t k_s)s + k_s k_t = 0 \tag{3.6}$$

By equating equation 3.6 with equation 3.5, a function can be formulated between ω, ζ and the suspension parameters which could further be used to investigate the effect of suspension parameters on ζ and ω of sprung and unsprung masses.

Also, referring back to the problem statement, the new 2-DoF system should have the same frequency for sprung mass and same overshoot, so,

$$\omega_1 = \omega_{ref} \tag{3.7}$$

$$\zeta_1 = \zeta_{ref} \tag{3.8}$$

Substituting equations 3.7 and 3.8 in equation 3.5 and comparing with equation 3.6, stiffness and damping coefficient for the sprung mass could also be calculated, which

is a bit complex than the simple calculations as done for the 1-DoF system. Figure 3.3 shows the pole-zero map of the 2-DoF system.

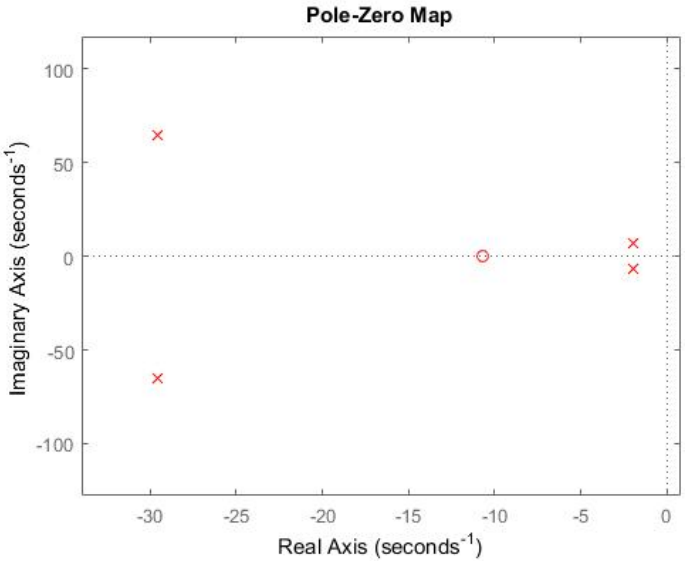

Figure 3.3: Poles of the 2-DoF reference syetem

3.2 Asymmetric Damper

All the simulations thus far were carried out with symmetric damper curves for compression and rebound. The analysis is now extended to an asymmetric damper curve with rebound force higher than compression force. The rebound and compression damping forces are considered to be individually linear. The load case investigated in this section is the step response. The load case is analysed for varying the slope of compression and rebound damping co-efficient. A comparison between these two variations is studied to understand the effect of varying parameters of damper curve on the different vibration modes of the vehicle.

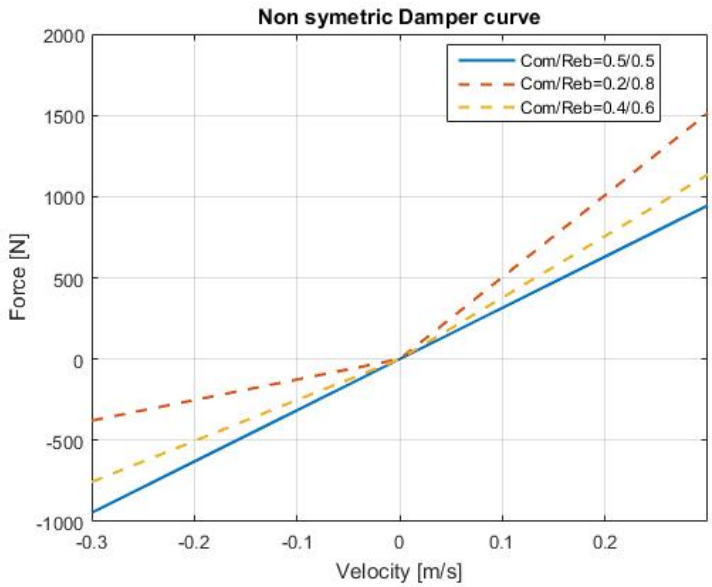

Figure 3.4: Damper curves analysed in simulations

The step response can be imagined to a physical scenario of encountering a bump on the road. The effect of asymmetry in the damper curve is expected to be more prominent in this load case since it is a transient input to the system. In this case, the time response is useful to analyse the behaviour of the system since the variation is easier to visualise and relate practically.

Simulations are carried out for the three sets of damper curves shown in Figure 3.4. The blue curve is a simple linear damper as discussed in the previous section and the two dotted curves are two asymmetric damper curves for two different combinations of compression to rebound ratio. A comparison between the three damper curves can be drawn since the average damping among the three dampers is kept the same. The metrics analysed are related to the sprung mass and the unsprung mass motion, which can then be related to ride and handling attributes of the vehicle.

3.3 Non-linear Symmetric Damper

The next step was to do the analysis of piece wise linear or symmetric non linear dampers which has been discussed in the introduction. As it is already known that velocity dependent non linear dampers have three variables viz.

- Low speed region
- High speed region
- Knee point

which could also be observed in Figure 3.5. The idea here is to analyse the effect of each of these three variables on the 2-DoF system. To start with, the same problem statement of matching the sprung mass response for different systems as discussed earlier is referred.

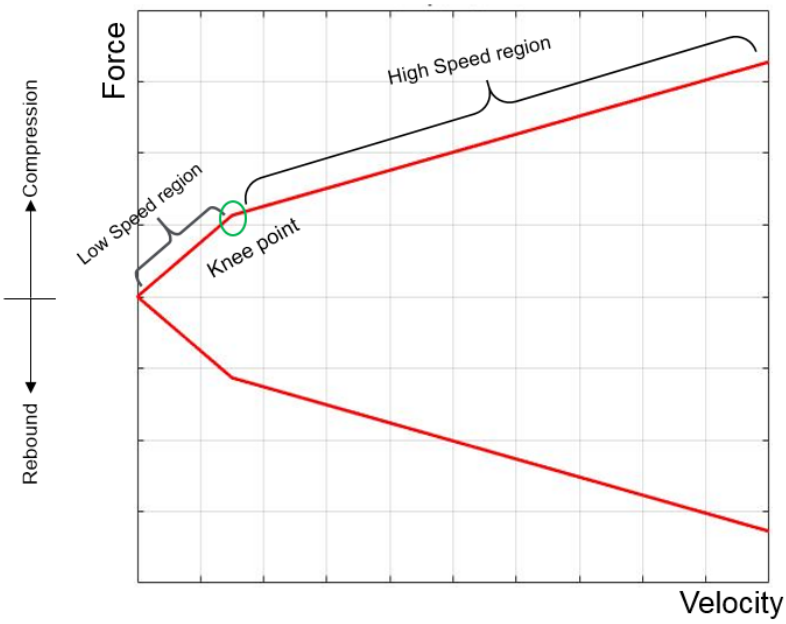

Figure 3.5: Non-linear symmetric (Piece-wise linear) damper curve

3.3.1 Matching Response

A step input of 0.05m amplitude is given to a 2-DoF system with parameters mentioned in Table 3.2. The sprung mass of the system is varied and the stiffness of the sprung mass is calculated using pole placement method as discussed before. To calculate the damping coefficient, low speed damping coefficient of the reference system (C_{LS-ref}) is used in the pole placement method to calculate the gain factor (equation 3.9), which is then multiplied by the reference high speed damping (C_{HS-ref}) to get a new high speed damping value (C_{HS-new}). Figure 3.6 shows the new damper curve for the new system with sprung mass being 1.2m.

$$gain factor = \frac{C_{LS-new}}{C_{LS-ref}} \tag{3.9}$$

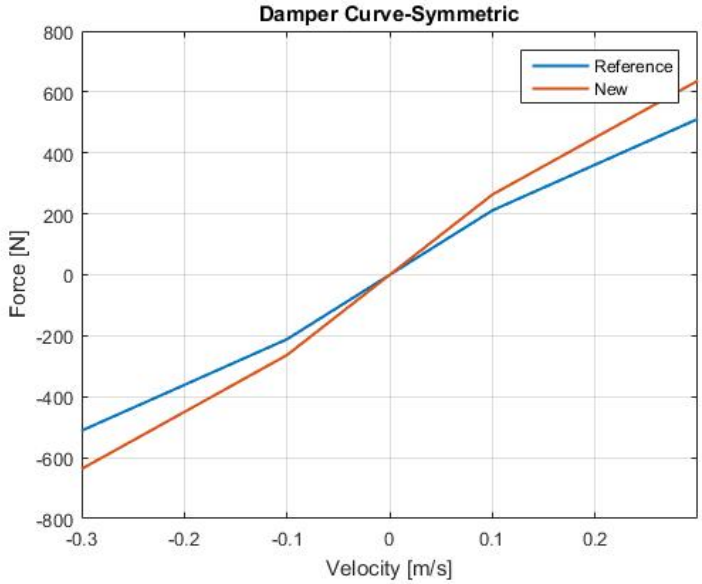

Figure 3.6: Non linear symmetric damper curve for new and reference system

Since, non-linear dampers are velocity dependent, the next step was to analyse the response over the velocity and frequency range. A sine sweep function, which has been discussed earlier, is used for this analysis. It is also important to understand the frequency response of these simulations and thus, bode plots for the sprung mass and unsprung mass displacement and acceleration is plotted. The $'tfestimate'$ function was used to calculate the amplitude and phase of the time-domain signals. As discussed in Section 2.5.2, the input sine sweep function over a time period of 200 seconds and frequency varying from 0-20 Hz (Figure 2.6) is used as the road disturbance.

3.3.2 Varying Slope of Low Speed Damping

To study the effect of varying the slope of damping co-efficient in the low speed region, the same simulation was carried out for the sine sweep input. The different damper curves considered for the simulations are shown in Figure 3.7. The input to the system remains the same decaying amplitude-increasing frequency sinusoidal signal from Section 2.5.2 (Figure 2.6). By varying the slope of the low speed damping co-efficient, it can be seen that the slope of the high-speed damping co-efficient also varies, though the slope of the high speed damping co-efficient is kept constant.

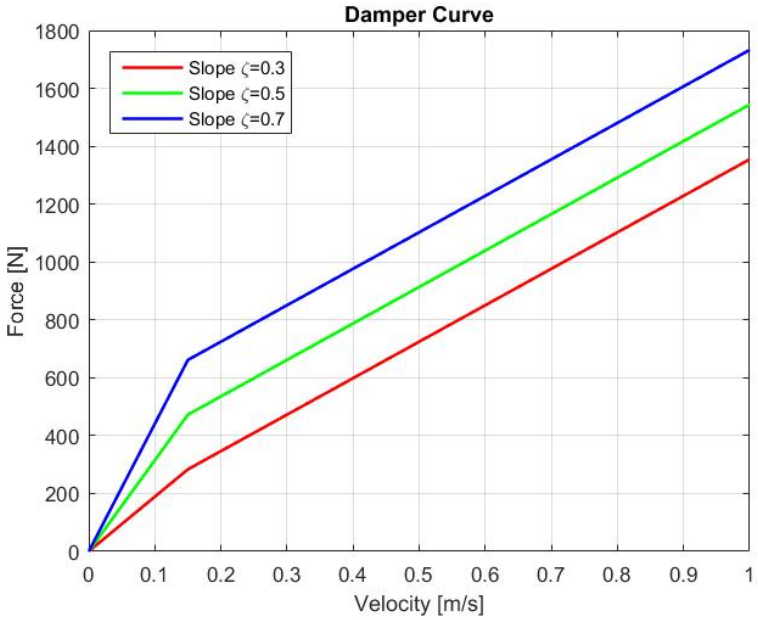

Figure 3.7: Damper curves for varying slope of low speed damping co-efficient

The frequency response of the sprung mass displacement for the three damper curves is also calculated using the $tfestimate$ function. Similar bode plots for other metrics of interest such as sprung mass acceleration and unsprung mass displacement are also obtained.

3.3.3 Varying Slope of High Speed Damping

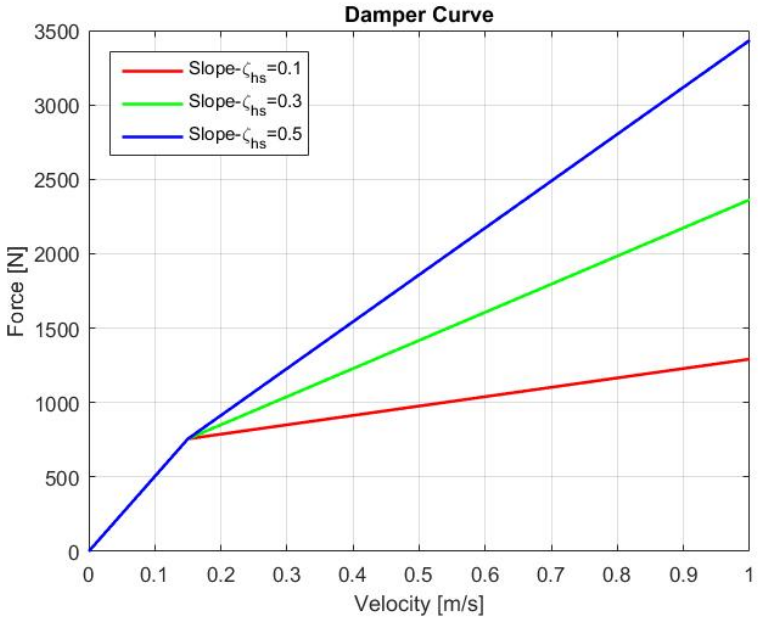

Figure 3.8: Damper curves for varying slope of high speed damping co-efficient

This analysis carried out using the sine sweep input to understand the effects of varying the slope of the high speed damping region. Since the high speed damping region is considered to be a high frequency event and the excitation of the unsprung mass occurs in the high frequency region, varying the high speed damping is important to understand the behaviour of the unsprung mass mainly and also to check the effect on sprung mass, if any. In this section, the slope of the high speed damping co-efficient is varied and simulation is performed similar to the previous section. The damper curves considered in this section are shown in Figure 3.8. Bode plots for the sprung mass and the unsprung mass metrics were obtained similar to the previous sections for each damper curve.

3.3.4 Varying Knee Point

The third parameter in consideration with the damper curve is the knee point, or the transition point between the low speed and the high speed regions. The knee point is varied and effectively, the high speed damping is also varied. Figure 3.9 shows the damper curves for varying knee point.

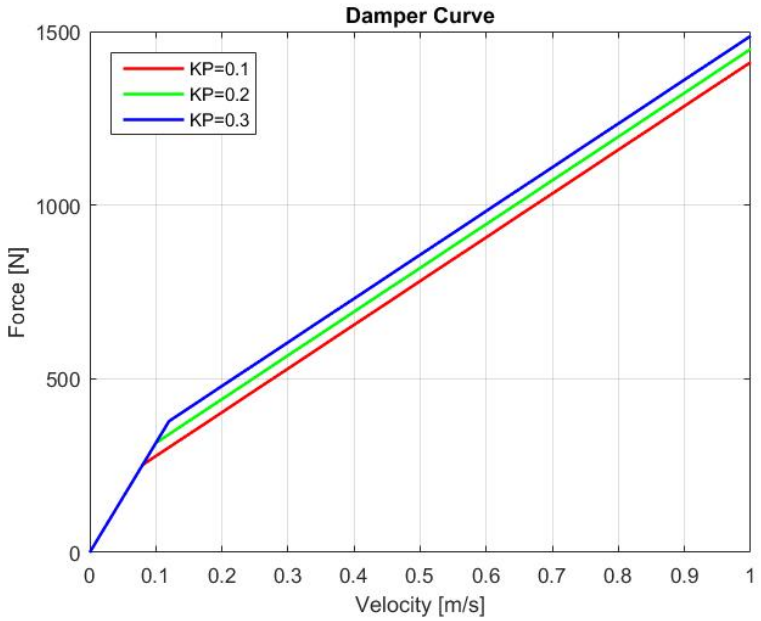

Figure 3.9: Damper curves for varying knee point

3.3.5 Sensitivity Analysis

From the above section it could be seen that varying Low-speed damping is affecting high-speed damping as well, and so is the case when knee point is varied. Hence, analysing the effect of each variable individually is not possible in this manner. So, a sensitivity analysis (Design of experiment) is discussed in this section where all the three test factors are varied with two test levels (i.e. high and low), information of which is given in Table 3.4. This would result in 8 unique combinations of tests

with the help of which the influence of individual factors and also combinations of them could be observed.

Table 3.4: Three factor test with two levels of each factor

Factors	**Low(-1)**	**High(+1)**
Slope-Low speed damping(LS)	0.3	0.8
Slope-High speed damping(HS)	0.1	0.5
Knee point (KP)(m/s)	0.05	0.15

Eight unique combinations of the three factors are shown in Figure 3.10. Bode plots are established for all these eight combinations and then each bode plot is divided into four sectors based on frequency:

- 0 to 1 Hz (Low velocity range): During simulations with the swept sine wave, it was observed that if the frequency is within 1 Hz, which is below the natural frequency of sprung mass, the damper velocity was low and usually within the knee point velocity, and could be considered as low velocity region.
- 1 to 3 Hz: This frequency range is dominated by the sprung mass natural frequency hence, analysing this sector separately gives a clear understanding of the requirements around the sprung mass natural frequency.
- 3 to 8 Hz: Mid frequency range
- 8 to 15 Hz: High frequency range: This sector is dominated by the natural frequency of unsprung mass system.

HS	LS	HS*LS	KP	HS*KP	LS*KP	HS*LS*KP
-1	-1	1	-1	1	1	-1
1	-1	-1	-1	-1	1	1
-1	1	-1	-1	1	-1	1
1	1	1	-1	-1	-1	-1
-1	-1	1	1	-1	-1	1
1	-1	-1	1	1	-1	-1
-1	1	-1	1	-1	1	-1
1	1	1	1	1	1	1

Figure 3.10: Factorial test with eight combinations

The same sensitivity analysis is performed for acceleration metrics as well. Figure 3.11 shows a schematic diagram of the whole setup for which the analysis is done.

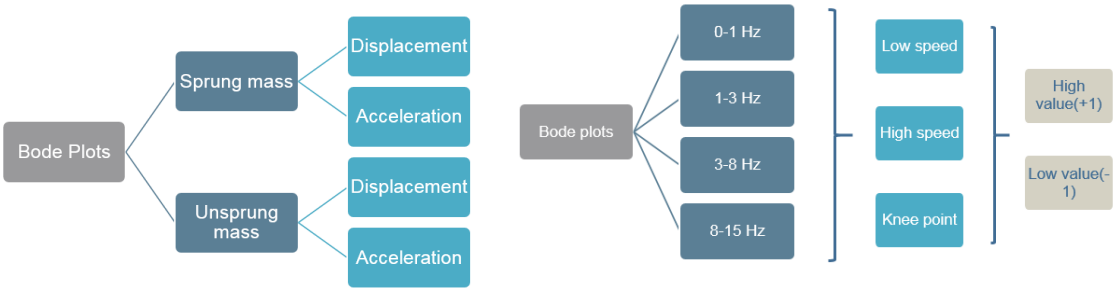

(a) Bode plots **(b)** Schematic of DoE analysis

Figure 3.11: Schematic diagram of DoE analysis

3.4 Non-linear Asymmetric Damper

After the analysis of linear asymmetric and non-linear symmetric dampers, in this section asymmetricity is added to the non-linear damper. Sine sweep input function is not used here for the analysis since the average damping for both symmetric and asymmetric damper is supposed to be the same, so it is hard to visualise the influence of asymmetricity. Also, the effect of asymmetric dampers has already been discussed in section 3.2, so this section is used to analyse the influence of knee point on asymmetric non-linear dampers. Step function is used as the input in this analysis. Figure 3.12 shows the force-velocity curve for a asymmetric damper with varying knee points and its influence on 2-DoF system is discussed in the conclusion section.

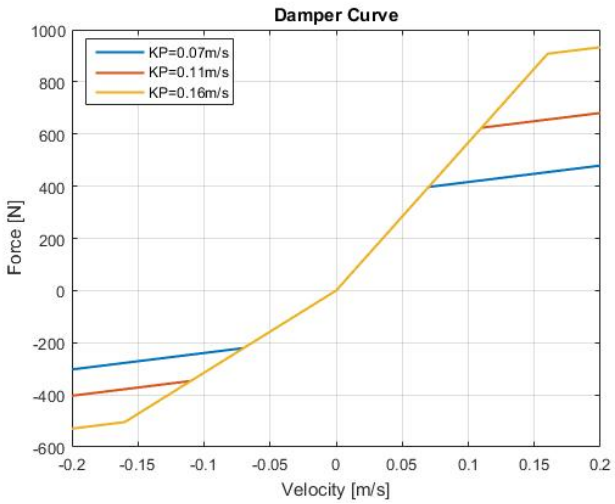

Figure 3.12: Force velocity plot with varying knee point

3.5 Comparison of linear, asymmetric and asymmetric dampers with knee point

The behavior of sprung and unsprung mass is compared for the three types of dampers by giving step input. Figure 3.13 shows the three damper curves

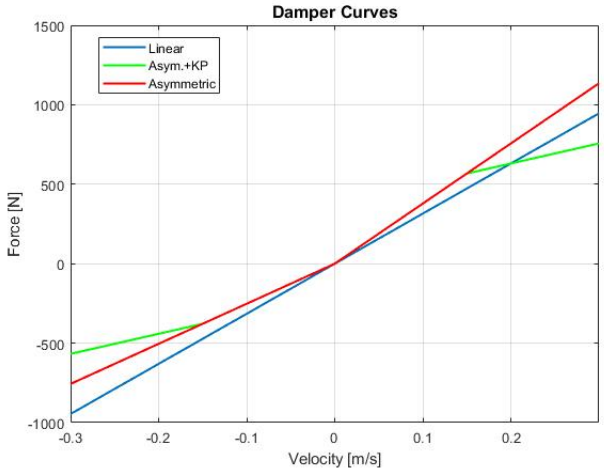

Figure 3.13: Force-velocity plot for dampers

In figure 3.13, the force-velocity slope for linear damper is considered to be 0.5 here. For asymmetric damper, it is 0.6 for rebound and 0.4 for compression. For asymmetric damper with knee point, the slope for high speed damping is considered to be 0.3.

3.6 Half-car Roll Analysis

Figure 2.3 shows a half-car model which has been used to investigate the effect of damping on the roll mode of the half-car. For simplicity, the anti-roll bar has been excluded and also the half-car is considered to be perfectly symmetric with centre of gravity being at the centre. The effect of suspension geometry has also been excluded. Hence the idea here is to get some basic understanding about the effect of damping on the roll motion of the car.

Input to the half car model are two sine waves with increasing frequency and decreasing amplitude which are out-of-phase with each other as shown in Figure 3.14. The values of all the parameters for half car could be seen from Table A.1 in appendix. This as a result initiates a roll motion in the half-car without initiating any bounce motion due to symmetricity of the half-car model. Hence, the effect of roll motion could be analysed independently.

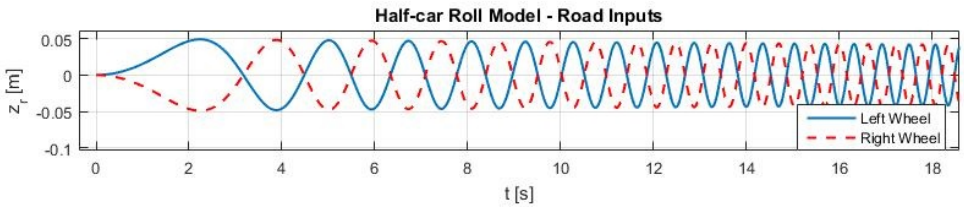

Figure 3.14: Input to the half-car model

A sensitivity analysis as discussed in section 3.3.5 has been used to understand the influence of damping factors in different frequency sectors, the results of which are discussed in the results section 4.

4
Results

The findings from the previous chapter are explained in this chapter. The damping requirement is drawn based on the analyses performed earlier. The metrics analysed for the different dampers are unique in this study since the idea here was to identify the key metrics for different operating regions.

4.1 Linear Damper and Pole Placement

4.1.1 1-DoF Quarter Car Poles Analysis

The idea of obtaining the same response for two different systems by matching the poles of the system provided a different way of looking at the quarter-car model. The procedure was straightforward for a 1-DoF system since the equations could be solved analytically. So, if the damping coefficient of the new system is as per equation 3.4, the new system will have the poles on the same location and hence the response for a step input function for varying mass will also be the same as can be seen in Figure 4.1.

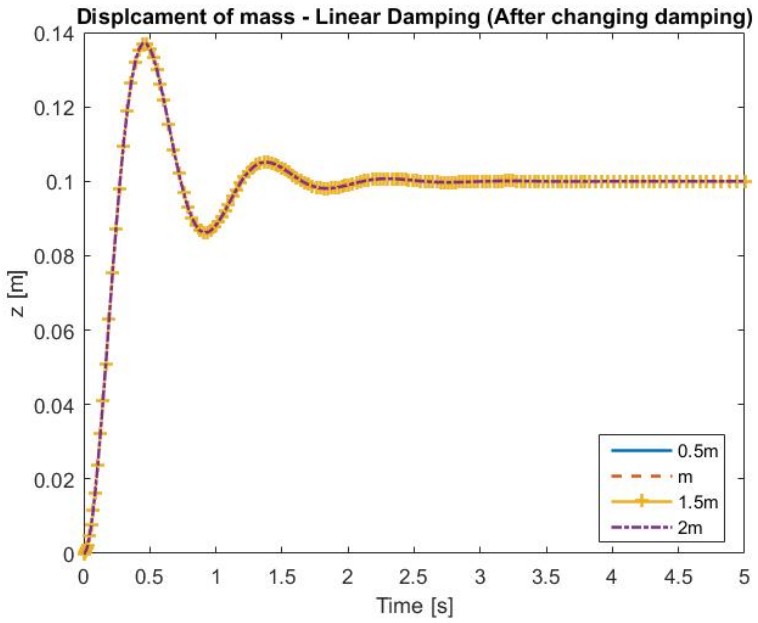

Figure 4.1: Step response of 1-DoF system

The 1-DoF model provides a good picture of the behaviour of sprung mass analysis but it ignores the behaviour of unsprung mass system. It is seen in case of a 1-DoF quarter-car model, matching the poles of two different systems is straight-forward in a way that the new damping value of the system is simply the mass ratio multiplied by the reference damping value. For a 1-DoF system,

$$c_{new} = \frac{m_{new}}{m_{ref}} c_{ref} \tag{4.1}$$

The downside is that this method cannot be used for a 2-DoF model as the equations for the pole of 2-DoF model is fourth order and it is hard to find an explicit equation for the same.

4.1.2 2-DoF Quarter Car Poles

It is discussed in Section 3.1.2 that the pole placement method could provide accurate results when the same response for two different systems is desired for a quarter-car 2-DoF model. The gain from the pole placement method is that it provides information regarding the behaviour of the sprung mass and the unsprung mass individually for changes in the suspension parameters. The analytic expressions for the relationship between the different parameters is valid only for a 1-DoF linear system and cannot be used for a 2-DoF system. It is also complex to form explicit analytic expression for ω and ζ for a 2 DoF system, hence MATLAB has been used to do the same. The dependence of the different parameters can be seen graphically from the results obtained from the pole-placement method.

Figure 4.2a shows the poles and zero of the 2-DoF system but the interesting plot is Figure 4.2b, where the poles of the 1-DoF model are compared with the poles of the 2-DoF model.

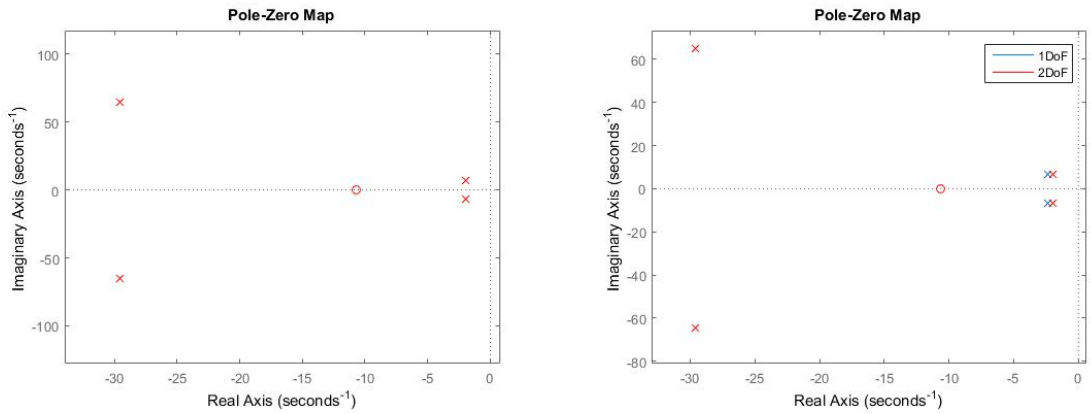

(a) Pole-zero map of 2-DoF system **(b)** Comparison with poles of 1-DoF system

Figure 4.2: Pole-zero map

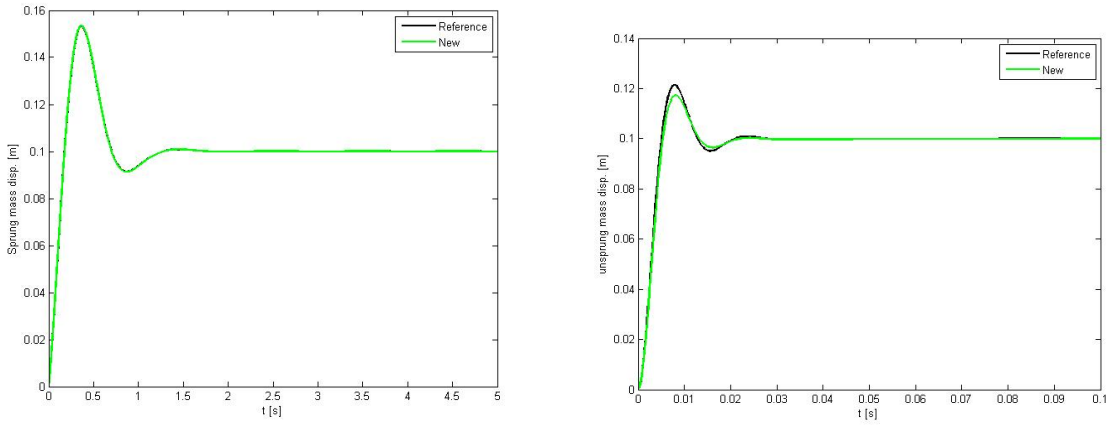

(a) Displacement of sprung mass **(b)** Displacement of unsprung mass

Figure 4.3: Step response of 2DoF system

Figure 4.3 shows the response of 2 DoF system. The sprung mass response is matching the response of reference system but variations can be seen in the unsprung mass response. Also, the time axis in Figure 4.3b is 0.1 second because the response of unsprung mass system for step input is fast due to the fact that poles of unsprung mass system are far away from origin (Figure 4.2b) and so the time axis is also magnified to visualize the effects in a better way.

To further investigate the behaviour of unsprung mass, case discussed in section 1.4 is simulated. Figure 4.4 shows the plots for variation of four different parameters for varying the sprung mass keeping the unsprung mass constant for a 2-DoF system and it is desired that the natural frequency is same for all the mass ratio combinations. From the plots, it can be seen that increasing the sprung mass by keeping the same natural frequency and to obtain the same response,

- The damping ratio of the unsrpung mass increases.
- The natural frequency of the unsrpung mass increases.

Since the analysis is performed on a linear quarter-car model with a linear damper, the results obtained show a linear trend. These results were obtained by solving the expression for the transfer function of the 2-DoF quarter-car model using the symbolic toolbox in Matlab and hence it is difficult to provide the relationship in terms of expressions. The same reasoning can be used to explain the results in Figure 4.5.

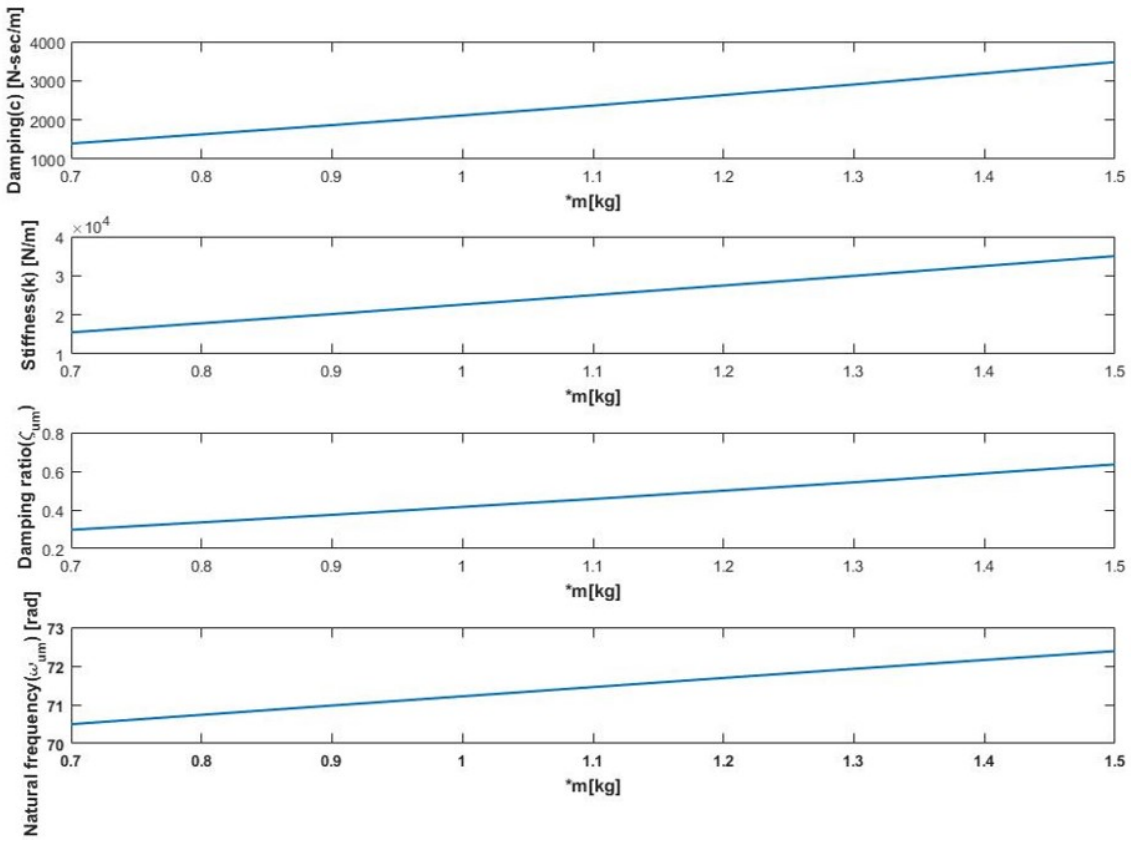

Figure 4.4: Variation in parameters for varying mass ratio

The next step was to see the effect of varying the damping on sprung and unsprung masses. Hence variatiion in damping is taken along the x axis. Figure 4.5 shows the variation of the sprung mass natural frequency, unsprung mass natural frequency and unsprung mass damping for variation in sprung mass damping. The interesting results from these plots are -

For increasing the damping co-efficient of sprung mass

- Increases natural frequency of sprung mass
- Decreases natural frequency of unsprung mass
- Increases damping of unsprung mass system to a point that unsprung mass system might become over-damp.

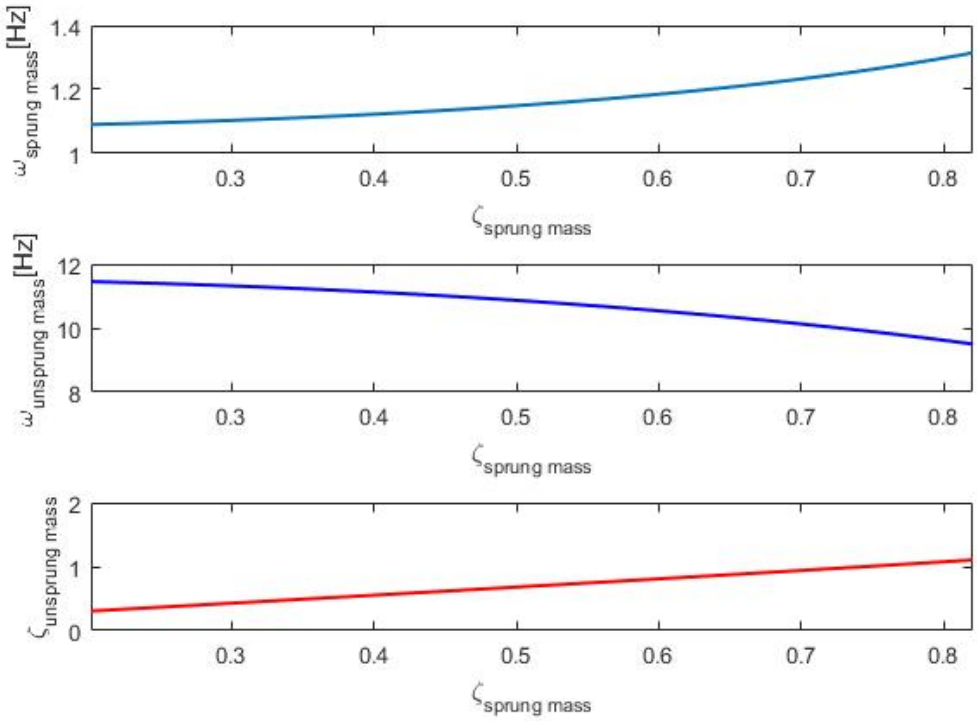

Figure 4.5: Variation in parameters for varying sprung mass damping

4.2 Asymmetric Damper

Simulations were performed with asymmetric dampers for a positive step input to study the effect of asymmetricity by investigating metrics of interest for the sprung and unsprung masses.

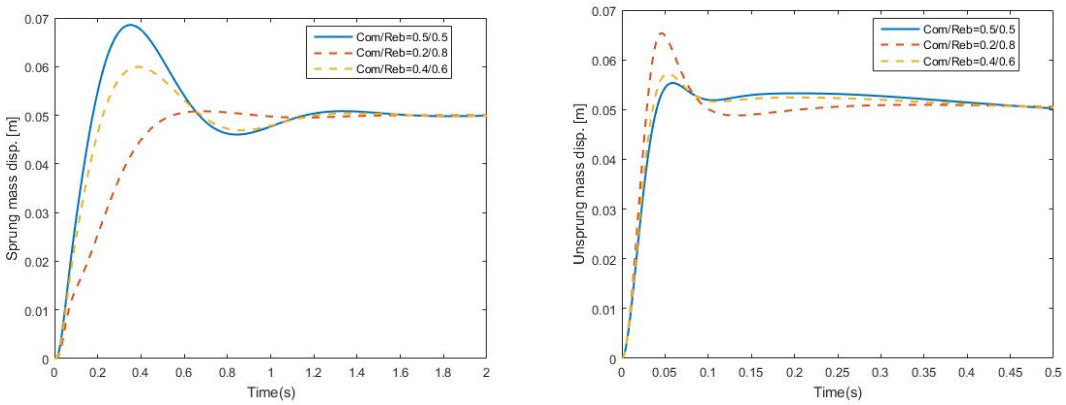

(a) Sprung mass displacement **(b)** Unsprung mass displacement

Figure 4.6: Asymmetric damper - Displacement Response

Figure 4.6 shows the displacement response plots of the sprung mass and the un-

sprung mass. It can be seen that the damper curve with the highest rebound damping slope has the lowest peak displacement value for the sprung mass and vice-versa for the unsprung mass.

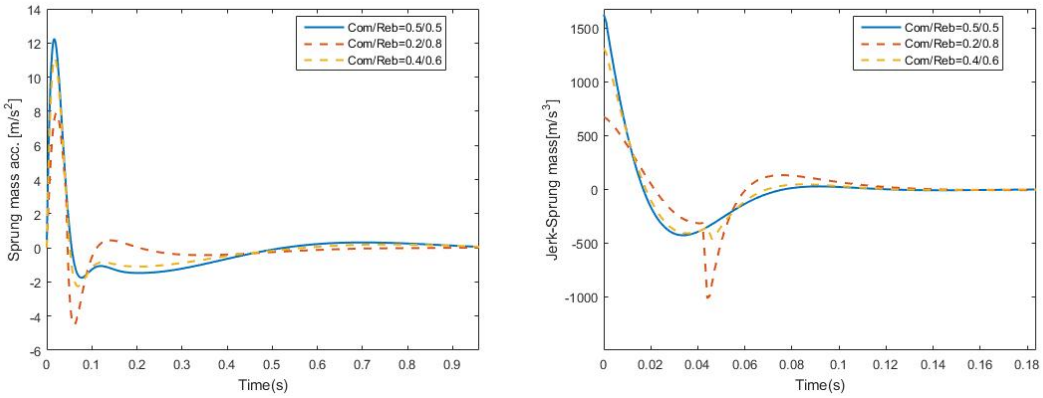

(a) Sprung mass acceleration **(b)** Sprung mass jerk

Figure 4.7: Asymmetric damper - Acceleration and Jerk Response

In Figure 4.7a, it can be seen that the asymmetric damper with the highest rebound force has the lowest absolute peak value. Another parameter to consider here is the settling time, which corresponds to the vehicle settling at it's equilibrium position after encountering a bump. The settling time is also faster for the damper with the highest rebound force.

Conclusions cannot to be drawn for the reason behind the asymmetric nature of the damper curve just by analysing the displacement plots. In order to establish a more comprehensive motivation, the sprung mass acceleration and jerk plots in Figure 4.7 are analysed. Jerk is the time derivative of acceleration and can be related to the actual feeling of the passengers in the cabin. It is seen that the damper with highest rebound damping has the lowest initial peak value. The sharp peak seen at 0.04s is due to the transition between the compression and rebound forces at the origin. Since a simplified damper curve is used for the simulation, the sharpness at the origin causes the peak value to fluctuate during the transition.

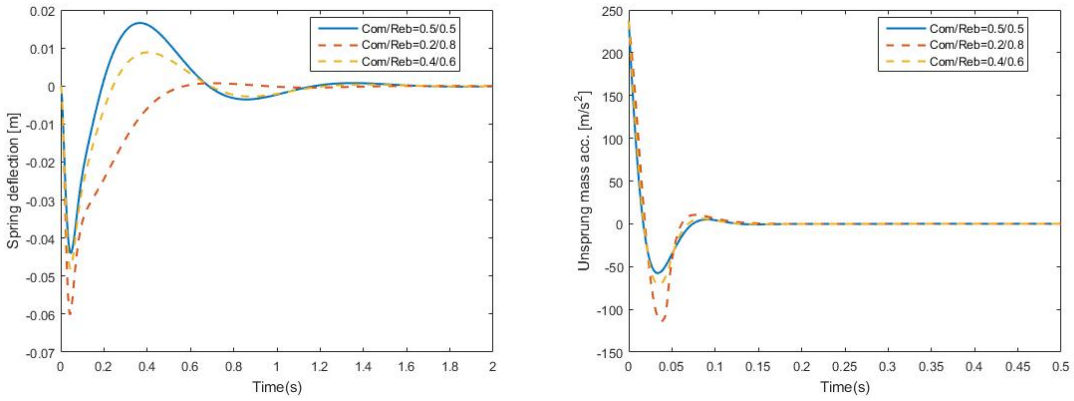

(a) Spring deflection **(b)** Unsprung mass acceleration

Figure 4.8: Limiting Metrics for Asymmetric Damper

The spring deflections and unsprung mass metrics shown in Figure 4.8 are important to understand the limiting factors for the asymmetric damper since there is usually a constraint on the amount of spring travel and the unsprung mass acceleration can be attributed to handling characteristics.

The dotted red line in Figure 4.8a has the highest peak value, which corresponds to the damper with the highest asymmetricity and a similar trend is seen for the unsprung mass acceleration in Figure 4.8b.

4.3 Non-linear Symmetric Damper

The fundamental idea behind performing simulations with non-linear dampers was to look into the frequency domain response of the performed simulations. A bode plot of the sprung mass displacement obtained from a simulation for varying the slope of the low speed damping region is shown in Figure 4.9. Similar bode plots were obtained for different metrics for varying all three parameters of the damper curve.

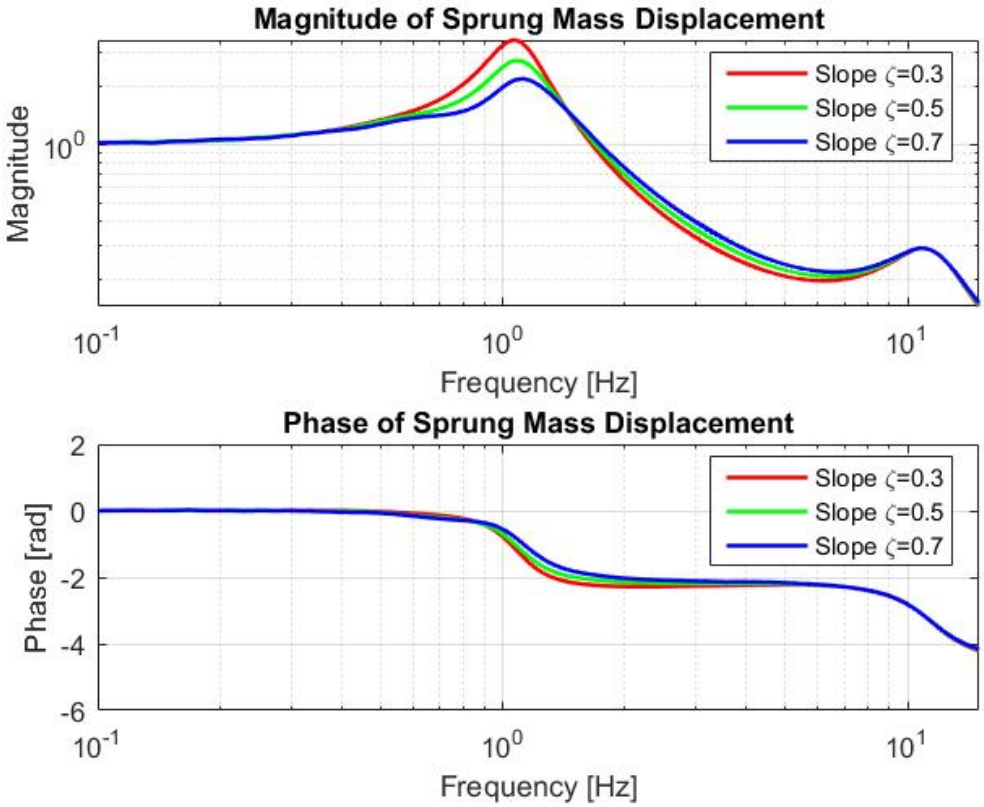

Figure 4.9: Frequency response of sprung mass displacement for varying slope of low speed damping co-efficient

4.3.1 Step and sine sweep response matching

As explained in section 3.3.1, the desired outcome of having the same response for the sprung mass for varying the mass ratio and keeping the same natural frequency was established. The results obtained from the linear model pole placement method were used to obtain the damping values for the non-linear system. It is seen in Figure 4.10a that the sprung mass displacement for the step input matches quite closely with each other. The unsprung mass displacement however, does not match with the reference system.

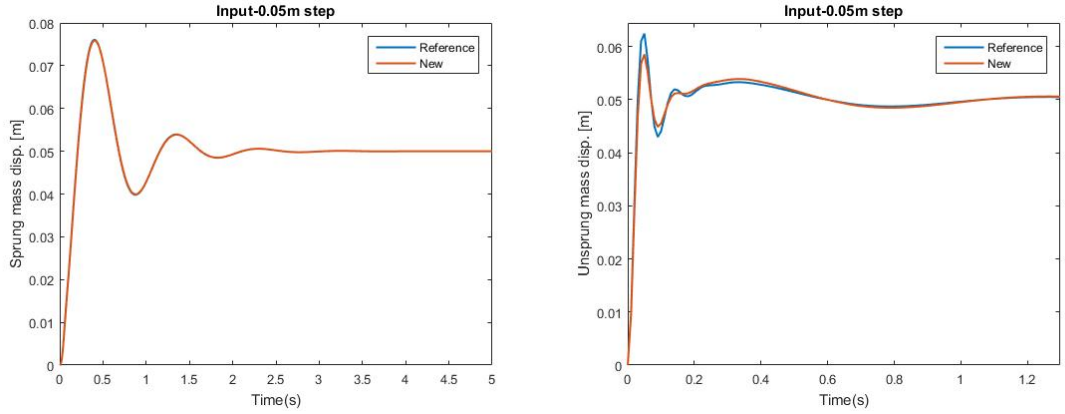

(a) Sprung mass displacement **(b)** Unsprung mass displacement

Figure 4.10: Nonlinear symmetric damper - Displacement Response

The same analysis was carried out for a sine sweep input and the same trend was observed. The sprung mass displacement matches with the reference system and the discrepancies in the unsprung mass behaviour can be observed (Figure 4.11).

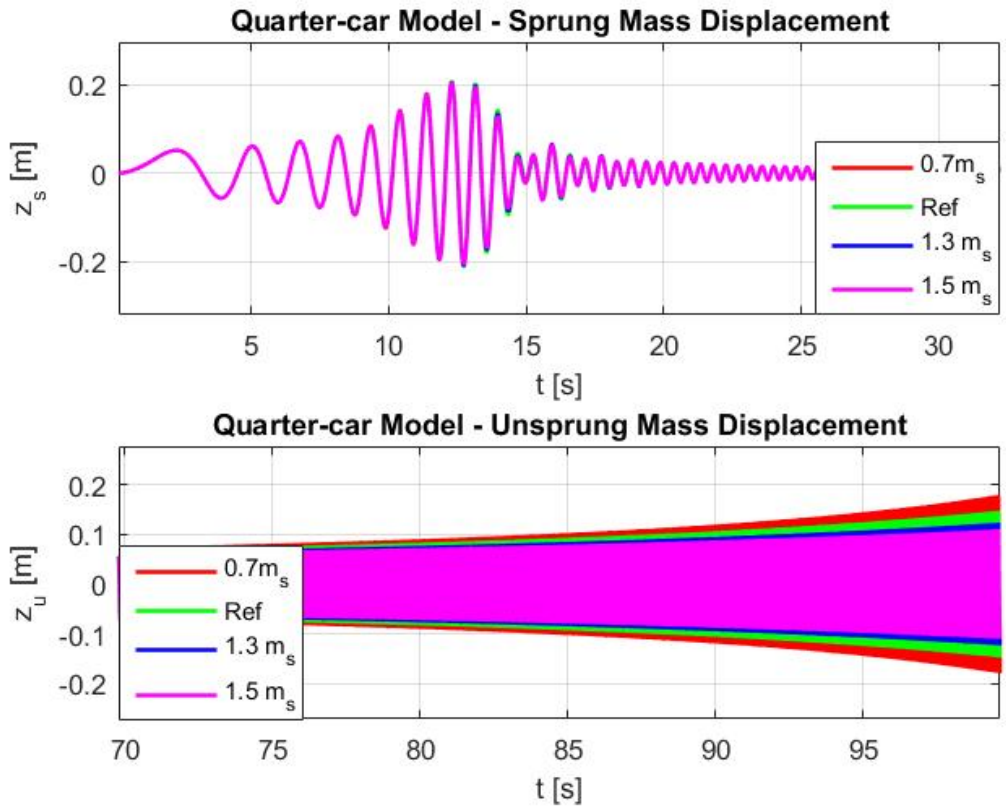

Figure 4.11: Sine sweep displacement response

The frequency response for non-linear systems changes with the input amplitude. In this case of the non-linear damper, exciting the system below the knee-point makes

the system behave as an asymmetric damper. Thus it is useful to plot which part of the damper was active while analyzing the time history of the system response. Figure 4.12 shows the damper velocity for the same combination of sprung mass ratios. From this figure, we can see that the damper velocity crosses the knee point around $t = 9s$. We can also observe from Figure 4.13 that the system with $0.7m_s$ briefly crosses the knee point between $t = 7.9s$ and $t = 8.02s$. From these results, we can understand which part of the damper was active.

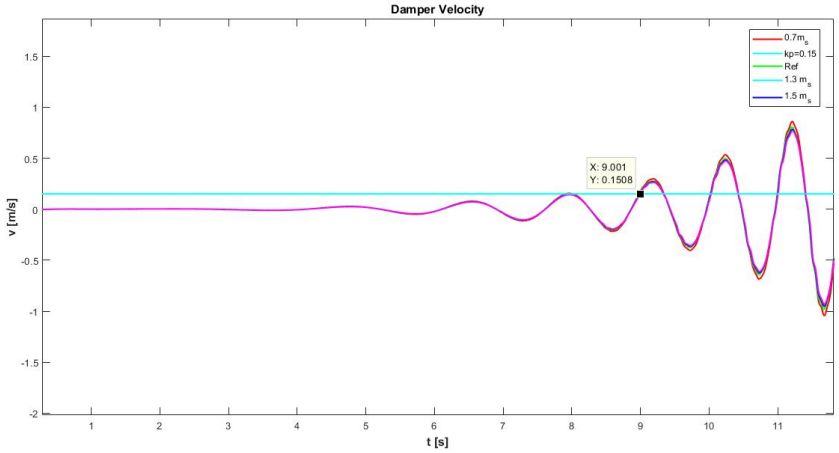

Figure 4.12: Damper Velocity for the sine sweep simulation

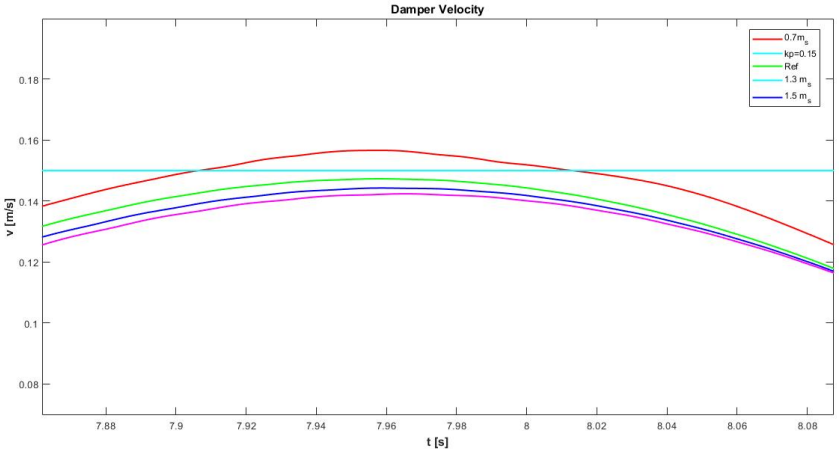

Figure 4.13: Damper Velocity for the sine sweep simulation - Zoomed section

A plot of the transfer function between sprung mass and input and unsprung mass and input is also plotted to analyse the behaviour over the frequency range. Here, in Figure 4.14, deviation is observed in the behaviour of sprung mass around 10Hz which is close to the natural frequency of unsprung mass system. Figure 4.15 shows the bode plot for the unsprung mass system.

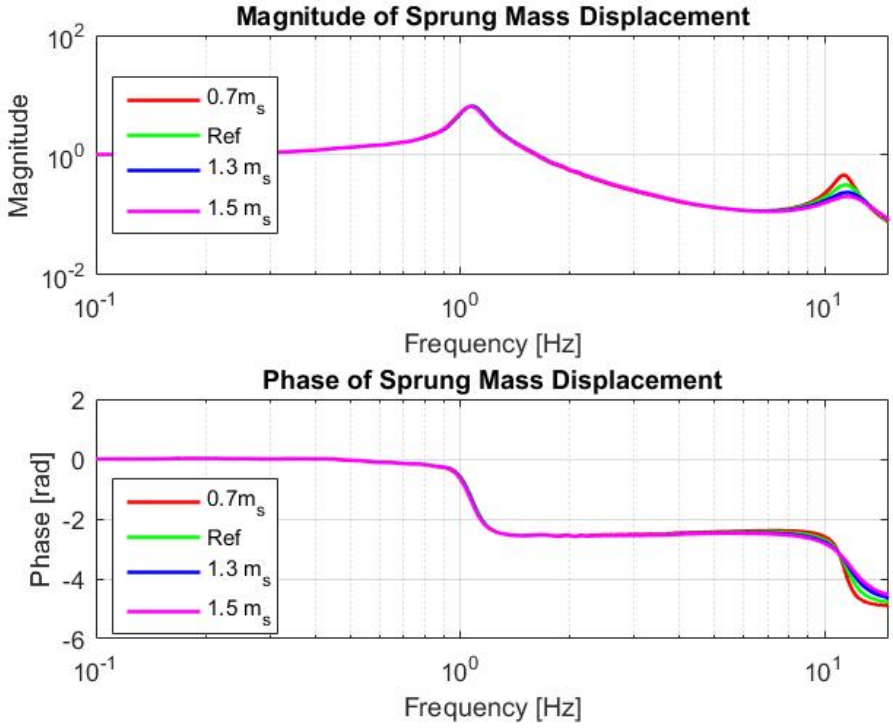

Figure 4.14: Bode plot- transfer function between sprung mass and input

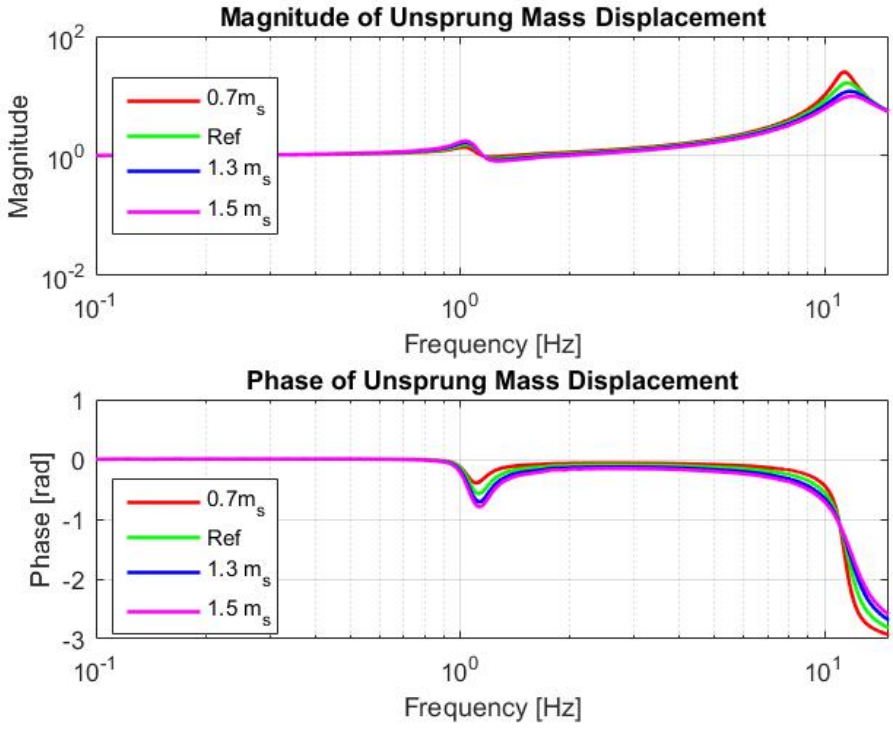

Figure 4.15: Bode plot- transfer function between unsprung mass and input

4.3.2 Effect of Damper Variables in Different Operating Regions

A sensitivity analysis is performed to highlight the effect of individual variables and a combination of variables on the frequency response. Based on the methodology in Section 3.3.5, this section discusses the results of DoE through Pareto charts. Figure 4.16 shows a DoE analysis for sprung mass displacement in the 0 to 1 Hz frequency range. The column to the extreme right is the RMS (root mean square) displacement for each of the settings. The highlighted row with the label 'Effect' shows the influence of each of the factor. The negative sign for HS and LS basically mean that with increase in damping for high and low speed will decrease the RMS displacement in the 0 to 1 Hz frequency range and the magnitude of this is used to plot the Pareto chart. The DoE analysis table for all frequency ranges are displayed in the appendix section.

	LOW Frequency-Unsprung mass(0-1)Hz							
	High speed	Low Speed		Knee point				
	HS	LS	HS*LS	KP	HS*KP	LS*KP	HS*LS*KP	RMS DISP
	-1	-1	1	-1	1	1	-1	1,1039
	1	-1	-1	-1	-1	1	1	1,0655
	-1	1	-1	-1	1	-1	1	1,0915
	1	1	1	-1	-1	-1	-1	1,0583
	-1	-1	1	1	-1	-1	1	1,089
	1	-1	-1	1	1	-1	-1	1,0699
	-1	1	-1	1	-1	1	-1	1,0565
	1	1	1	1	1	1	1	1,0558
Effect	-0,02285	-0,01655	0,0059	-0,012	0,01295	-0,00675	0,0033	
Magnitude	0,02285	0,01655	0,0059	0,012	0,01295	0,00675	0,0033	

Figure 4.16: DoE analysis table for sprung mass displacement

Pareto charts are derived for all the frequency sectors that has been discussed in Figure 4.16 for sprung and unsprung masses for non-linear symmetric dampers to see the effect of the variables dependently and independently of each other. Figure 4.17 shows the Pareto chart for the RMS of sprung and unsprung mass displacement in low frequency range (0-3 Hz). The magnitude of the effect is normalised to easily understand the degree of effect of other factors.

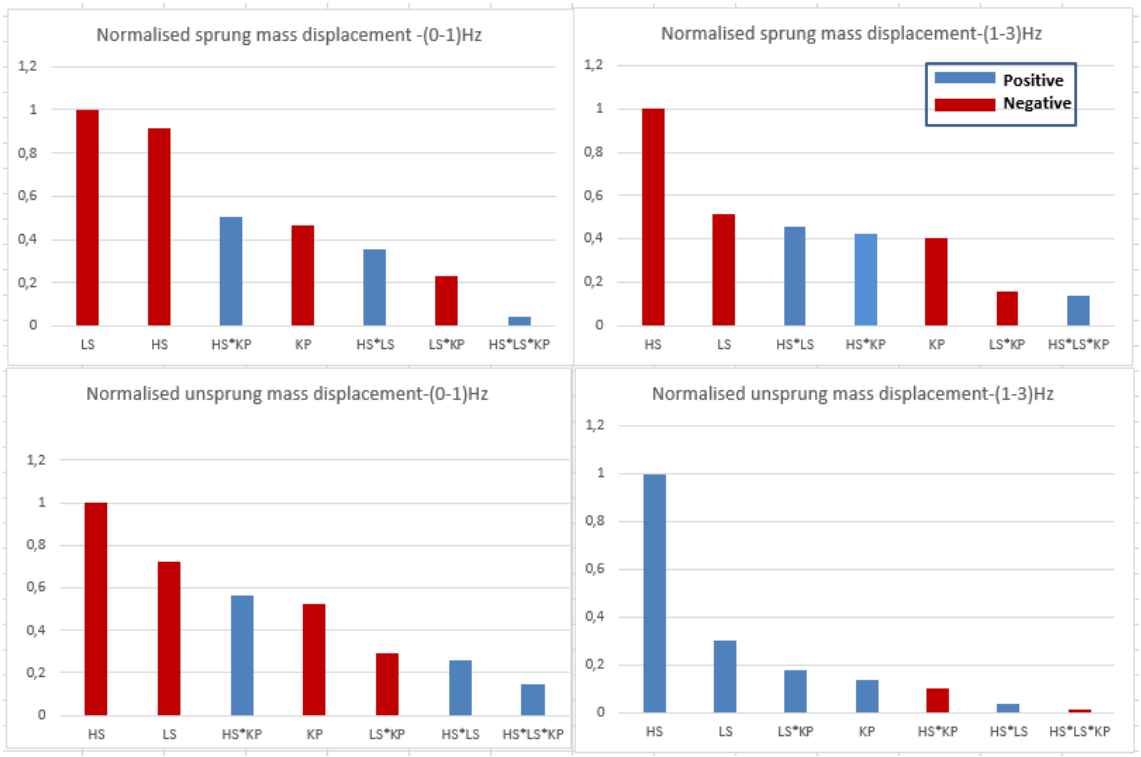

Figure 4.17: Pareto chart for sprung and unsprung mass displacement between 0-1Hz & 1-3Hz

Comparing the chart for sprung and unsprung mass between 0-1 Hz, it could be noticed that

- Influence of Low speed damping is maximum for sprung mass but for unsprung mass, it is HS damping.
- HS, LS damping and KP have negative effect i.e. increasing the values of these factors reduces the rms of displacement.
- Combined effect of HS & KP have a positive value, hence it could be a limiting factor for sprung and unsprung masses.

Similarly, comparison between 1 -3 Hz in Figure 4.17 shows

- This region is dominated by HS damping for both sprung and unsprung masses but having dissimilar effect
- For sprung mass, the effect is still negative but for unsprung mass the effect is positive i.e. increasing HS damping will increase the rms of displacement for unsprung mass.
- Effect of LS damping and other parameter is insignificant for unsprung mass because the effect is low.

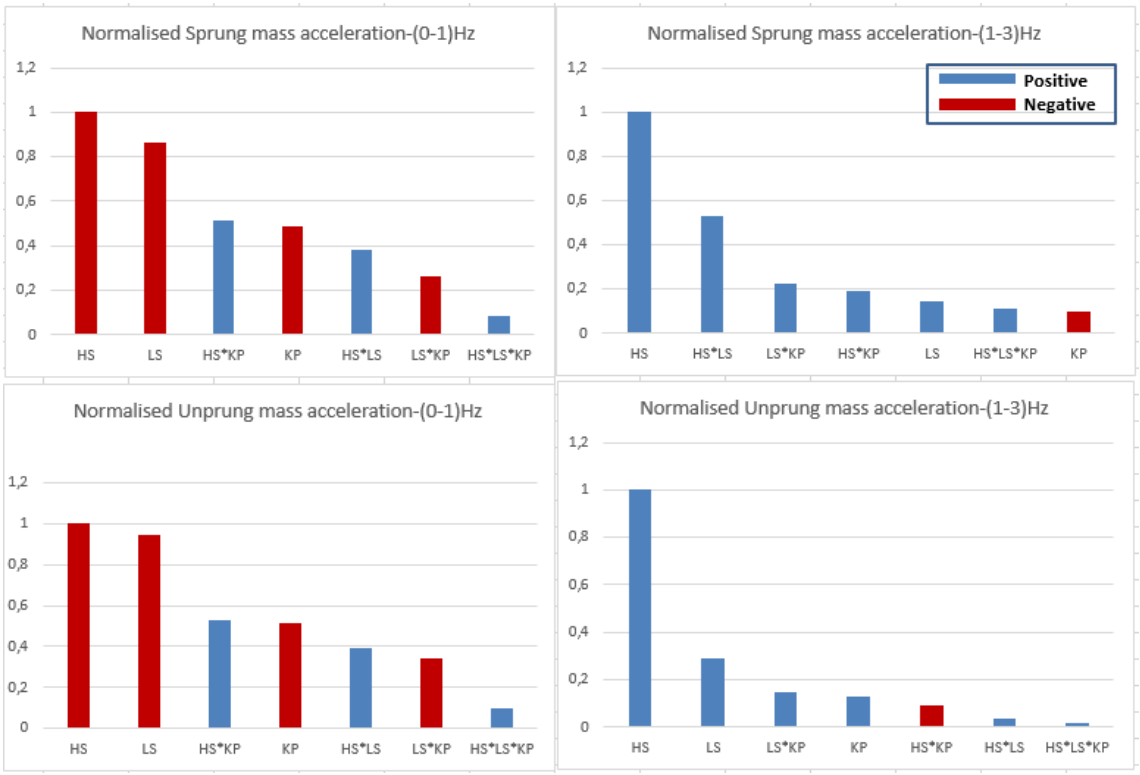

Figure 4.18: Pareto chart for sprung and unsprung mass acceleration between 0-1Hz & 1-3Hz

Figure 4.18 shows the Pareto chart for acceleration of sprung and unsprung masses in 0-3Hz frequency range. The important things to be observed here are

- HS damping is the dominant factor for both sprung and umsprung masses between 0-3 Hz range.
- Between 0-1 Hz, both HS & LS damping has negative effect and are dominant factors.
- Though the combined effect of HS & KP and HS & LS for sprung and unsprung masses respectively gives positive effect and could be a limiting factor.
- Between 1-3 Hz, HS damping is the most dominant factor and it has positive effect on acceleration, i.e increasing the HS damping will increase the rms acceleration for both sprung and unsprung masses.

After the analysis in lower frequency, Figure 4.19 shows the Pareto chart for displacement in mid and high frequency range.

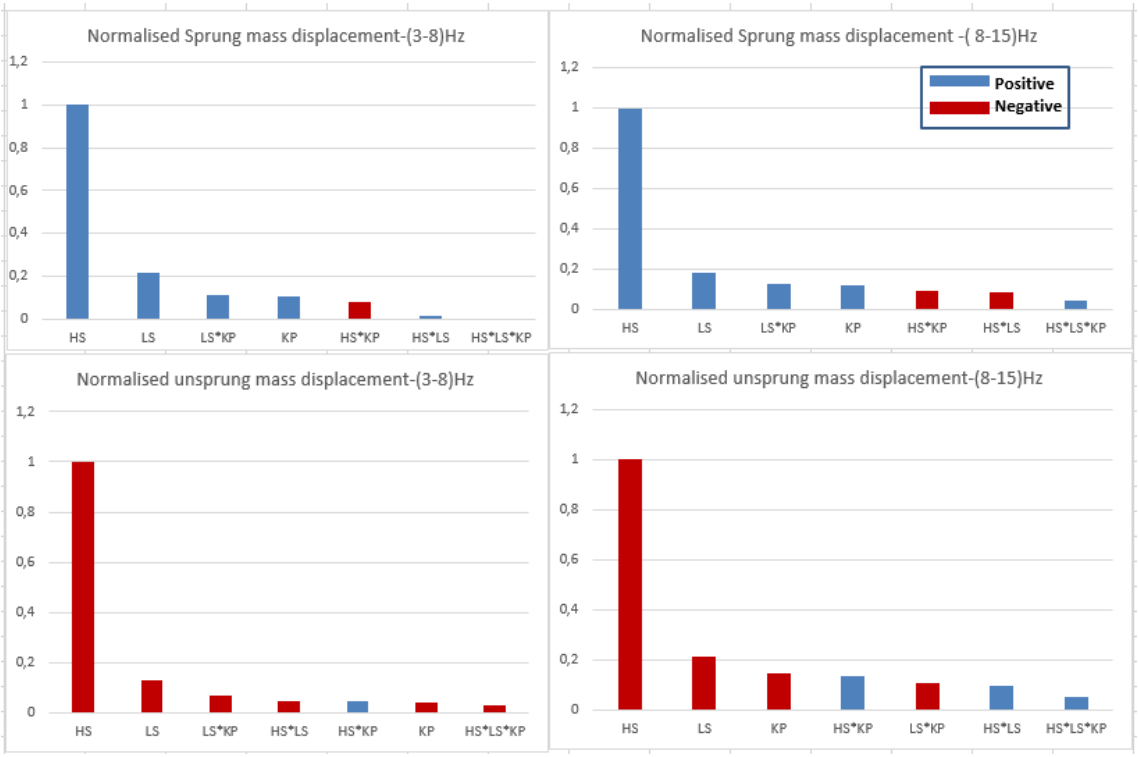

Figure 4.19: Pareto chart for sprung and unsprung mass displacement between 3-8Hz & 8-15Hz

- The effect of high speed damping is the most dominant factor for both the masses and the other factors could be neglected.

- For sprung mass, HS damping has positive effect in both frequency sectors (3-8 Hz & 8-15 Hz).

- Unsprung mass show negative behaviour i.e., increasing HS damping will decrease the RMS displacement for unsprung mass.

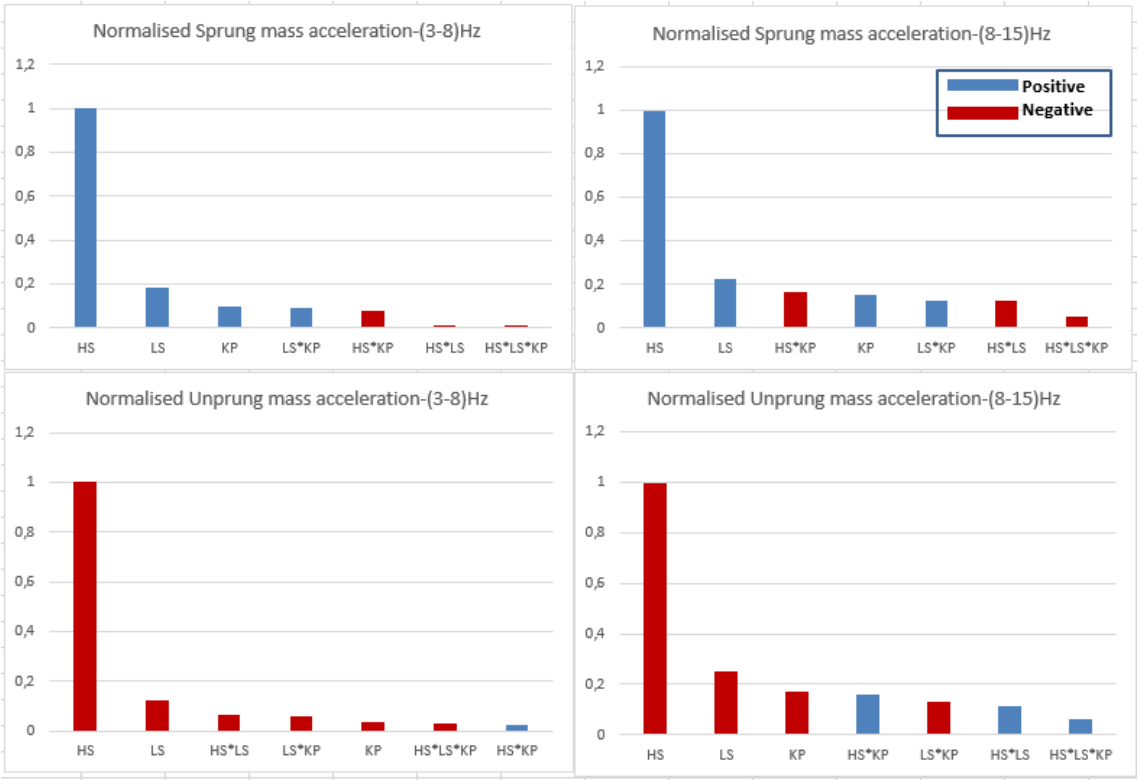

Figure 4.20: Pareto chart for sprung and unsprung mass acceleration between 3-8Hz & 8-15Hz

Figure 4.20 shows the Pareto chart for RMS acceleration from 3 to 15Hz. Following observations could be made through this plot:

- The behaviour is similar to the displacement chart as in Figure 4.19.
- HS damping is the dominant factor with dissimilar behaviour for sprung and unsprung masses.

4.4 Non-linear Asymmetric Damper

As discussed in section 3.4, a step input is used in this case to study the behaviour of sprung and unsprung mass and find the important factors which could effect the system. Figure 4.21 shows the response of sprung and unsprung masses of 2-DoF system. The results show that

- With increase in the value of knee point, the peak value and the settling time of sprung mass system decreases making the system more damped.
- The peak value of unsprung mass is not effected but settling time decreases with increase in knee point value.

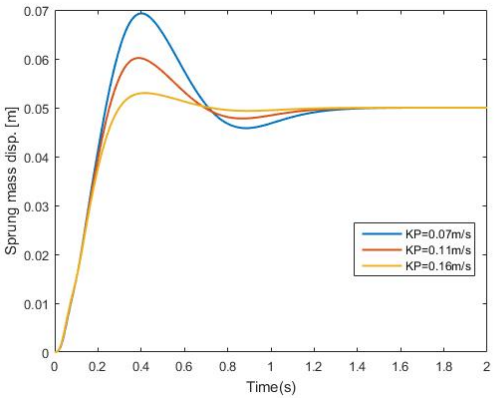

(a) Sprung mass displacement

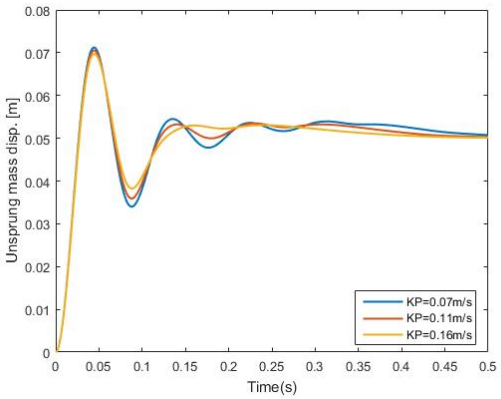

(b) Unsprung mass displacement

Figure 4.21: Response of a 2 DoF system

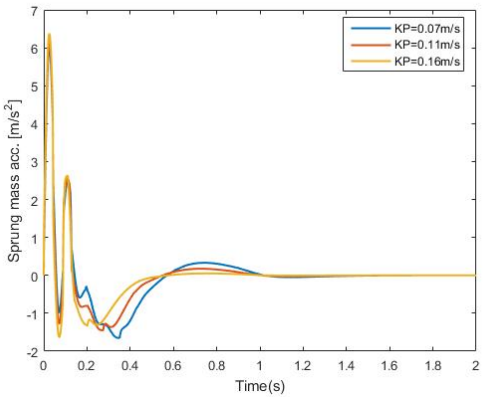

(a) Sprung mass acceleration

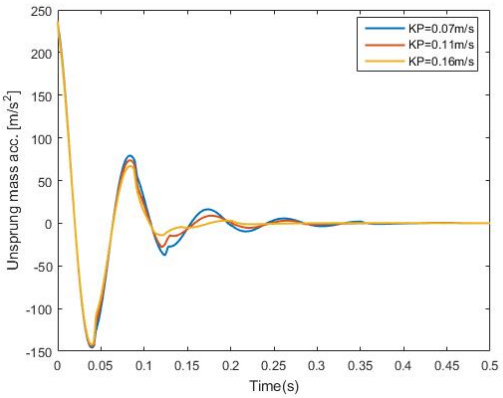

(b) Unsprung mass acceleration

Figure 4.22: Acceleration response of a 2 DoF system

The initial jerk for sprung and unsprung mass could be a limiting factors in this case, as it can be observed in Figure 4.23 that with increasing the knee point, the initial jerk value increases for both sprung and unsprung mass which is undesirable.

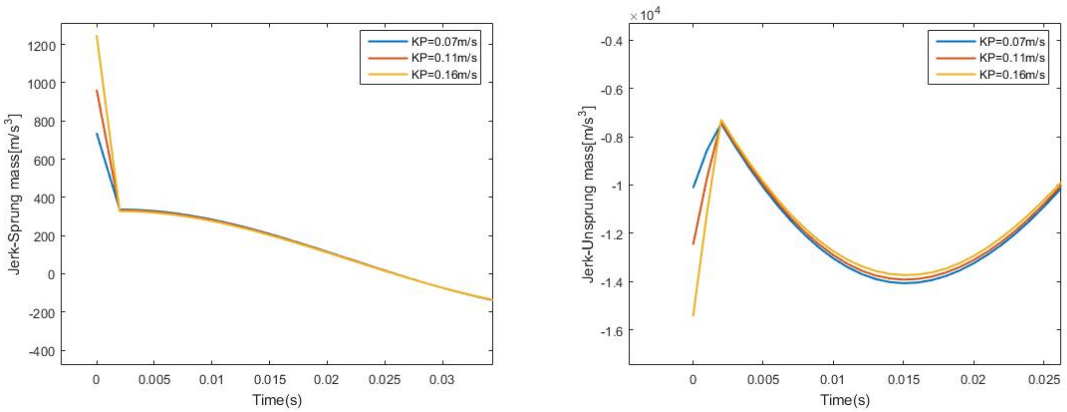

(a) Sprung mass jerk **(b)** Unsprung mass jerk

Figure 4.23: Jerk response of a 2 DoF system

4.5 Comparison of linear, asymmetric and asymmetric dampers with knee point

Step response of 2-DoF model is analysed based on the damper curve in Figure 3.13, the results of which are discussed below.

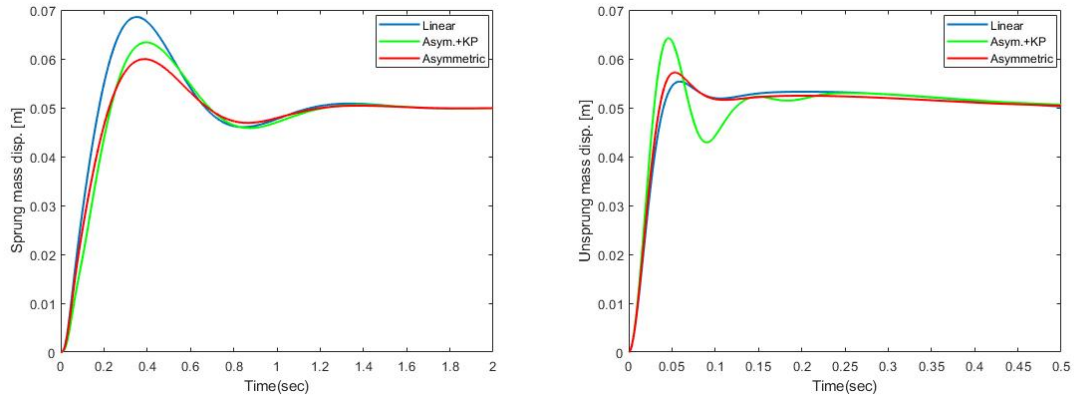

(a) Sprung mass displacement **(b)** Unsprung mass displacement

Figure 4.24: Displacement response of 2-DoF system for different dampers

For sprung mass displacement in Figure 4.24a, the overshoot is highest for the linear damper and lowest for asymmetric dampers without knee point. There is no significance difference in the settling time. In case of unsprung mass in Figure 4.24b, the highest overshoot is for asymmetric damper with knee point with further oscillations before it finally settles.

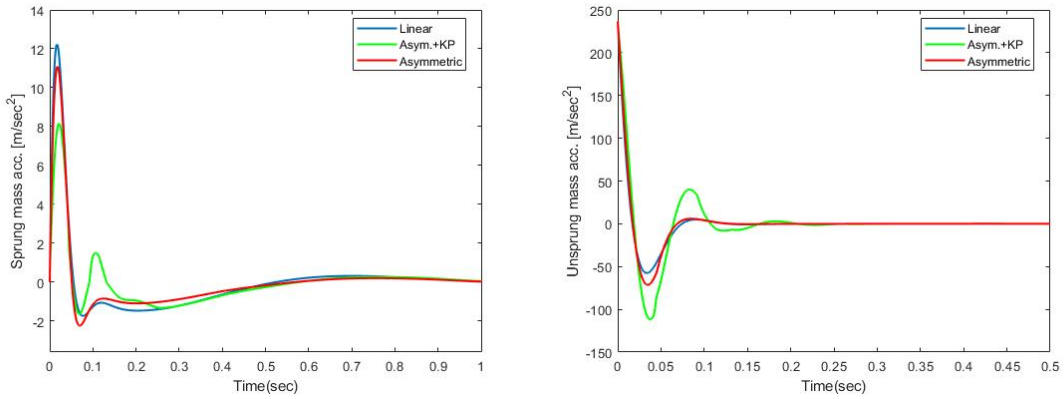

(a) Sprung mass acceleration **(b)** Unsprung mass acceleration

Figure 4.25: Acceleration response of a 2-DoF system for different dampers

In case of sprung mass acceleration in Figure 4.25a, the lowest peak acceleration is for asymmetric dampers with knee point and the highest is for linear dampers. In case of unsprung mass in Figure 4.25b, it is the opposite. Also, the settling time is highest for asymmetric damper with knee point.

4.6 Half-car Roll Analysis

Figure 4.26 shows the roll angle and roll acceleration of the sprung mass with the last plot being the unsprung mass acceleration of the half car model. It could be observed that the roll displacement attenuates to a really low value after around 25 seconds. It is not the same in the case of roll acceleration, this is due to the unsprung mass resonance at high frequency. A clear picture of this behaviour can be observed from the transfer function plots in Figure 4.27.

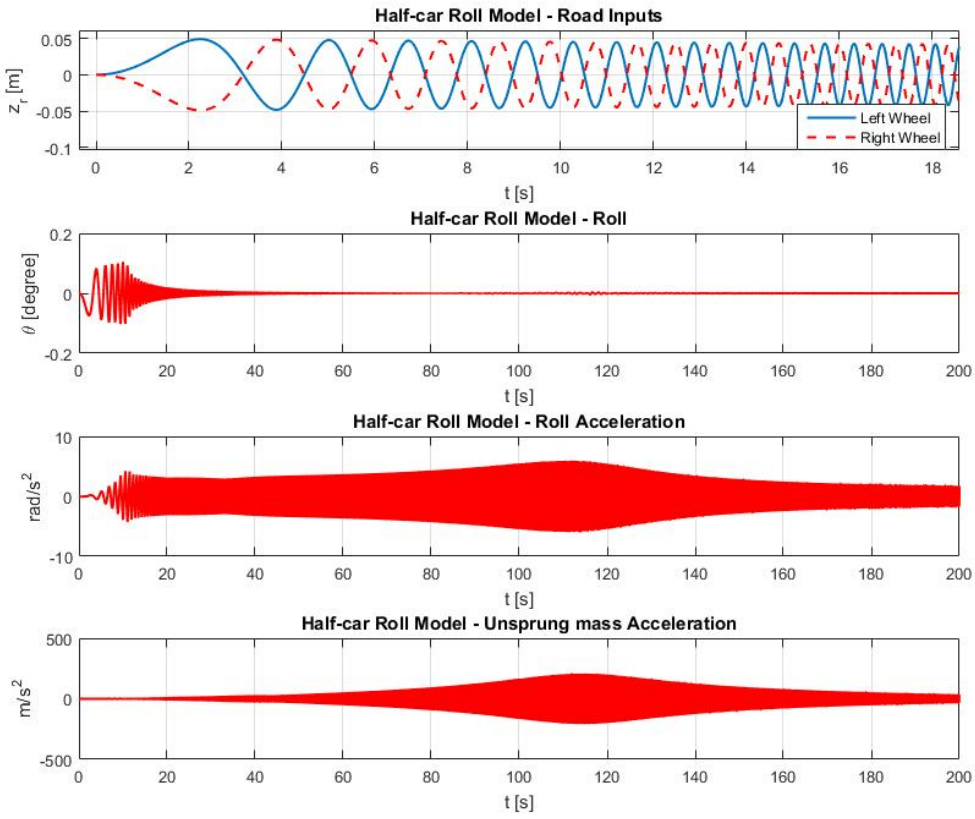

Figure 4.26: Half car response

In Figure 4.27a, peak of unsprung mass could be observed at high frequency due to resonance. The top plot is for sprung mass roll displacement and it could be seen that the magnitude goes really low at higher frequency but the magnitude of acceleration increases with frequency as is apparent from Figure 4.27b.

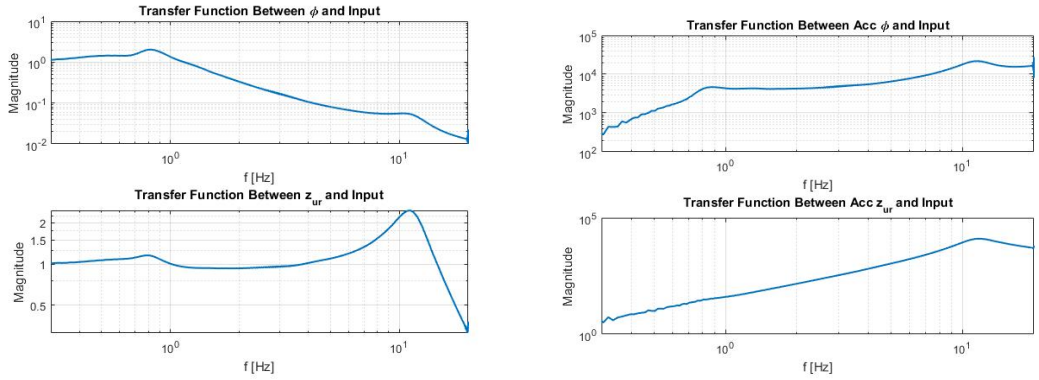

(a) Bode plots **(b)** Accelerations bode plots

Figure 4.27: Transfer function plots-Half car roll model

As has been discussed in section 3.6, the same procedure used for quarter-car model is used to investigate the influence of three factors (low speed damping, high speed damping and knee point) on the roll behaviour of half car.

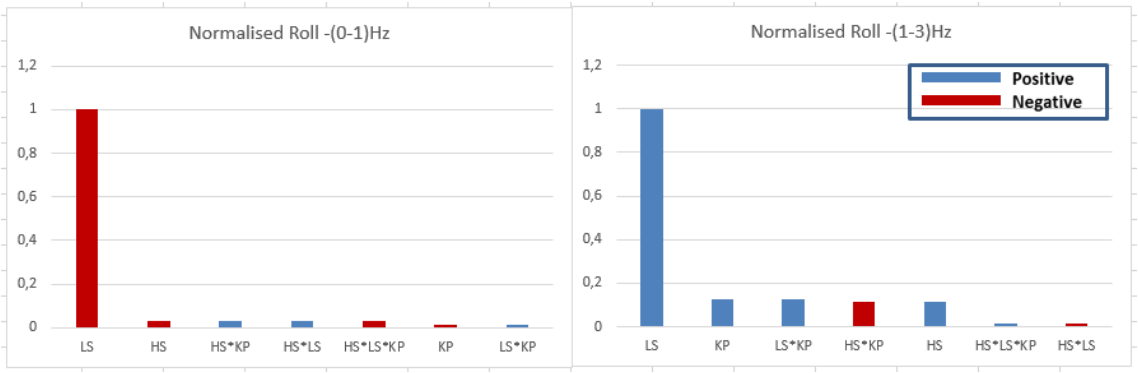

Figure 4.28: Pareto chart for sprung mass roll between 0-1Hz & 1-3Hz

Figure 4.28 shows the effect of different factors on roll angle of the half-car. It can be observed that

- Low speed damping is the major influencing factor here.
- Between 3-10 Hz, Pareto analysis is not considered for roll displacement since the magnitude was really low at those frequency as could also be seen in Figure 4.27.
- For low frequency (0-1Hz), a high damping value is required.
- From 1-3 Hz, the requirement is of low damping.

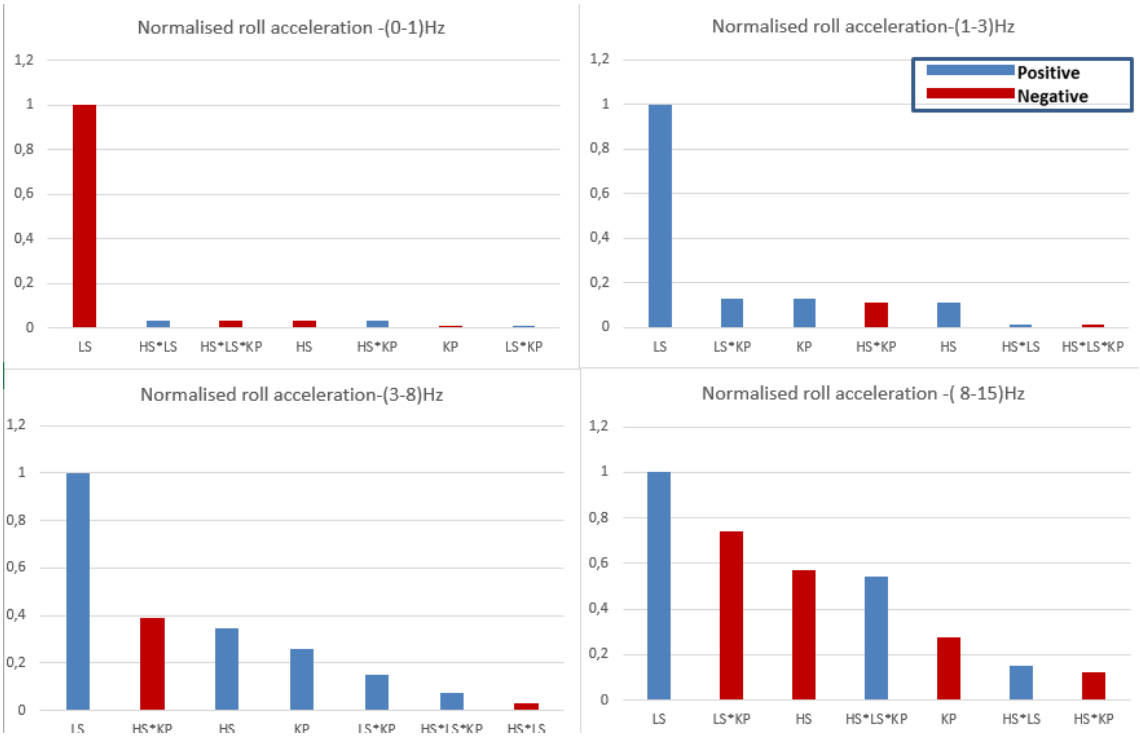

Figure 4.29: Pareto chart for sprung mass roll acceleration between 0-15Hz

Figure 4.29 is the Pareto for the factors affecting acceleration in the working frequency range from 0 to 15 Hz. It can be observed that

- LS damping is the influencing factor through out the frequency range.
- In 0-1 Hz range, a high value of LS damping is required.
- From 1-15 Hz, a low value of LS is preferred
- In higher frequency i.e. from 8-15 Hz, the requirement for LS and HS are contradictory.

5
Conclusions

This chapter discusses all the results that have been obtained in the previous chapter. Conclusion has been drawn from each section and finally a F-v curve is used to demonstrate the different requirement for sprung and unsprung masses.

5.1 Linear Damper

The results obtained from the pole-zero analysis carried out with linear dampers provide a lot of insight with respect to capturing the system behaviour with simple models.

For two 1-DoF quarter-car systems with different sprung masses, it is seen that the same response can be obtained by matching the poles of the two systems. The poles can be matched by varying the damping of the new system proportional to the mass ratio. The same methodology was applied to a 2-DoF quarter-car system to understand the behaviour of the unsprung mass along with the sprung mass. Results from section 4.1 show that the dominant poles of the 2-DoF system lie very close to the poles of the 1-DoF system for same sprung mass. These are the dominant poles and they characterise the sprung mass response more than the poles which are farther away from the imaginary axis. Thus, it can be seen that the sprung mass behaviour can be captured to a great detail with a simple 1-DoF quarter-car model but an advanced 2-DoF model is required to capture the unsprung mass behaviour.

The behaviour of unsprung mass for 2 DoF system is investigated further in section 4.1.2. It could be noticed that increasing the sprung mass effect the behaviour of unsprung mass as well, if the natural frequency is to be kept constant. Since, with the increment in sprung mass, the stiffness and damping of sprung mass also has to be increased to match the response, this also increases the reaction forces on unsprung mass and hence making the unsprung mass system more stiff and over damped. This is apparent from the plots as well where the frequency and damping values are increasing with the increase in sprung mass.

The effect of varying just the damping could also be seen in Figure 4.5. Here though the unsprung mass system become overdamped, the frequency of unsprung mass system decreases. This result can be related in a physical sense that as the damping is infinitely increased, the natural frequency of the sprung mass goes on increasing

and the natural frequency of the unsprung mass goes on decreasing such that both the masses have the same natural frequency and vibrate as a single unit. The important takeaway from this analysis is that the damping of the masses have to be increased for increase in sprung mass ratio by maintaining same natural frequency and response for the different systems. This means that the unsprung mass will be over-damped if the sprung mass is increased to a numerically larger value. Another insight obtained is that, the damping of the unsprung mass is also effected when damping of sprung mass system is increased and goes over-damped when the damping of the sprung mass is around 0.65 for the given model. As discussed before, this is not a desired result since an over-damped unsprung mass system decreases the handling performance of the vehicle significantly. It is to be noted that these numbers are not representative of any vehicle but the idea is to explain the behaviour of the sprung mass and the unsprung mass metrics for variation in suspension parameters.

5.2 Asymmetric Damper

The results obtained from the analysis performed in section 3.2 is discussed here. The reason behind carrying out simulations with asymmetric dampers was to investigate the effect of asymmetricity of dampers on the vehicle response. As seen from the plots in section 3.2, there is a definite advantage of having the asymmetric nature of damper curves with respect to the sprung mass metrics. This result is on expected lines and forms a motivation for the asymmetric nature of damper curve. However, the unsprung mass metrics require a higher damping in compression because of faster response (Figure 4.6b) and is thus compromised a bit.

The effects of the asymmetric nature of the damper curve are highlighted from the results obtained in section 4.2 using a step input. As predicted, the sprung mass motion is controlled by the rebound damping and the unsprung mass motion is controlled by the compression damping. This behaviour could be discussed through the position of poles for sprung and unsprung masses. Since the poles of unsprung mass system is further away from origin compared to sprung mass, it will react faster to the step input. Hence the unsprung mass compresses first with sprung mass still static. Therefore, the dampers have compression movement. From Figure 4.6, it could be seen that he unsprung mass reaches its peak at 0.05 second and for sprung mass it happens around 0.4 second. So, at the peak time of sprung mass, the unsprung mass has already reached equilibrium, so the relative motion between sprung and unsprung mass is rebound, hence this effect the behaviour of sprung mass. This can be seen from the plots that the damper with the highest rebound force has the lowest peak displacement, which is of course desirable from a vehicle response point of view. The behaviour of the unsprung mass displacement is contrary to the sprung mass, where the damper with the highest compression force has the lowest peak displacement.

Analysis of the sprung mass acceleration and jerk metrics also gave similar results which provides additional motivation for the asymmetric nature of the damper curve. A point of consideration here is regarding the degree of asymmetricity. Though it

is seen that a higher rebound damping force gives good results for the sprung mass metrics, a limiting factor has to be established for the compression to rebound ratio. This could be based on the metrics analysed in Figure 4.8. It can be seen that the absolute peak spring deflection goes on increasing for increasing the rebound damping and decreasing the compression damping to maintain the average damping. The same trend is observed with the unsprung mass acceleration. Since there is always a constraint on the amount of room available for the spring to compress before it hits the bump stop, this could be a strong limiting factor to decide the degree of asymmetricity.

This result signifies the fact that an asymmetric damper alone is not sufficient to have good control of both the sprung mass and the unsprung mass, and hence there is a need to have a more complex non-linear damper by which the unsprung mass could also be controlled.

5.3 Non-linear Symmetric & Asymmetric Damper

The first takeaway can be obtained from the study of matching the system response for the non-linear dampers. Since the results from the 2 DoF poles system were used for this analysis, it is seen that a linear 2-DoF system could be used to analyse the response of 2-DoF system with non-linear dampers.

With non-linear dampers, the main idea was to investigate the effect of velocity dependent damping region viz.(low speed region, high speed region and knee point) independently and dependently on the response of sprung and unsprung mass in terms of displacement and acceleration. It was not possible to vary one of these three factors and keep the other two constant so sensitivity analysis in done by using Design of Experiment (DoE) method.

A sensitivity analysis (Section 4.3.2) is performed over four different frequency ranges to have a better understanding of each of the three factors i.e. Low speed damping, High speed damping and knee point.

For the frequency region of 0-1 Hz, which is roughly just before the natural frequency of sprung mass system, it was observed that the damper velocity is low, hence the analysis of this section is focused mainly on the low speed damping effect. From the plots in Figure 4.17, it can be observed that both sprung and unsprung mass demanded high value of LS and HS damping for minimising acceleration and displacement. Hence, it can be concluded that a high damping force is required in low velocity region for low frequency inputs.

But around the natural frequency of sprung mass (1-3 Hz), because of sprung mass resonance, the magnitude of sprung mass displacement increases and hence the damper velocity, so the effect of HS damping become more prominent. Around this frequency range, the focus should be on reducing transmissiblity i.e. the sprung mass displacement with respect to the input, so focus should be on the factors influencing

the sprung mass displacement rather than acceleration since both the parameters have different requirements. Also, from Figure 4.17, it could be observed that higher damping is required to reduce the RMS of displacement of sprung mass but at the same time unsprung mass displacement needs a lower damping value.

So, the focus here should be mostly on minimising the sprung mass displacement to dampen the resonance. Hence, a higher damping value could be preferred at the cost of unsprung mass displacement and comfort of the car (sprung mass acceleration). A higher damping value could be obtained by increasing the value of the knee point or increasing the HS damping value.

For non-linear asymmetric dampers, the effect of the knee point has been discussed in section 4.4 using step input. Increasing the knee point increases the velocity range for low speed damping and thus provides higher damping forces for a longer velocity range. This as a result decreases the peak value or overshoot of the sprung mass system but no effect could be seen on the overshoot of unsprung mass system. This is because the velocity of unsprung mass when it hits the step goes really high compared to knee point and sprung mass speed. But, the effect could be seen on the settling time of unsprung mass. This is also due to the fact that the low amplitude oscillations corresponds to low velocity damper region and if the low velocity range increases, the system will be damped fast thus decreasing the settling time.

However increasing the knee point and thus increasing the damping force has negative effect as well. From Figure 4.23, it could be observed that initial jerk value increases because of the higher high damping force region. Also, high velocity corresponds to high frequency inputs and for higher frequency, the aim should be mostly to isolate the sprung mass system to provide better comfort for the passenger. So, the focus should be on reducing the RMS of acceleration rather than displacement. From Figure 4.19, it could be observed that sprung and unsprung mass have contradictory requirement. To have better isolation, sprung mass system needs a lower high speed damping but for good handling unsprung mass system need higher value of the same. So a compromise is made based on the vehicle requirement with more focus towards reducing the acceleration level of sprung mass system to have better passenger cabin isolation.

Increasing the knee point does not effect the peak value of sprung and unsprung mass acceleration but the settling time decreases with increasing the knee point as could be observed in Figure 4.22. Based on the above discussion, it could be concluded that increasing the knee point decreases the settling time and the peak value thus suggesting a higher knee point.

5.4 Comparison of different dampers

The effect of rebound damping force could be seen in the sprung mass displacement behavior. Since the rebound force is highest for asymmetric damper without knee point (Figure 3.13), the overshoot is the lowest. When it comes to unsprung mass,

it is dominated by the compression damping force. The compression damping force is low for both asymmetric dampers and asymmetric dampers with knee point but because of the knee point, it is lowered down further and since the damper velocity around the overshoot is high enough to cross the knee point, the magnitude of overshoot is highest for the asymmetric damper with knee point (Figure 4.24).

When it comes to the acceleration of sprung mass, it is basically affected by the transfer of force through the unsprung mass when it hits the step input. For asymmetric damper with knee point, the compression force is the lowest, so when it encounters the step input, the force transmitted from unsprung mass to sprung mass is the lowest compared to other two types of dampers. Hence, asymmetric damper with knee point will provide better isolation from the road disturbances (Figure 4.25a). For unsprung mass, the acceleration of asymmetric damper with knee point is highest for the same reason. Since, the compression force is highest for the linear damper, it transfer the forces to sprung mass and hence results in low acceleration for unsprung mass (Figure 4.25b). So from this comparison study, it could be concluded that asymmetric dampers with knee point will provide better isolation to sprung mass but at the same time it will affect the ride characteristic due to high acceleration of unsprung mass.

5.5 Half car-Roll analysis

After the analysis of the 2-DoF quarter car model,a 4-DoF half car model is analysed in section 3.6 to see the influence of damping factors on roll behaviour of car. Close to the roll natural frequency, the requirement is to dampen the high amplitude, hence a high damping value is preferred. The roll displacement for mid and high frequency is really low so it can be ignored.

When it comes to acceleration, it could be observed in Figure 4.29 that LS damping has the major effect here as well but for higher frequency input, low damping value is preferred to isolate the sprung mass from roll disturbance. This is similar to the behaviour of sprung mass system bounce behaviour which needs lower damping at high frequency to isolate the sprung mass system.

5.6 Damping Requirement

Finally, to sum up the whole section, Figure 5.1 shows a depiction of the damper Force-velocity plot, which could help visualise the sprung mass and unsprung mass requirements in different velocity and frequency ranges. The curve is divided into low and high damping values. Green and red lines show damping requirements for sprung and unsprung mass respectively in different frequency zones based on the above results.

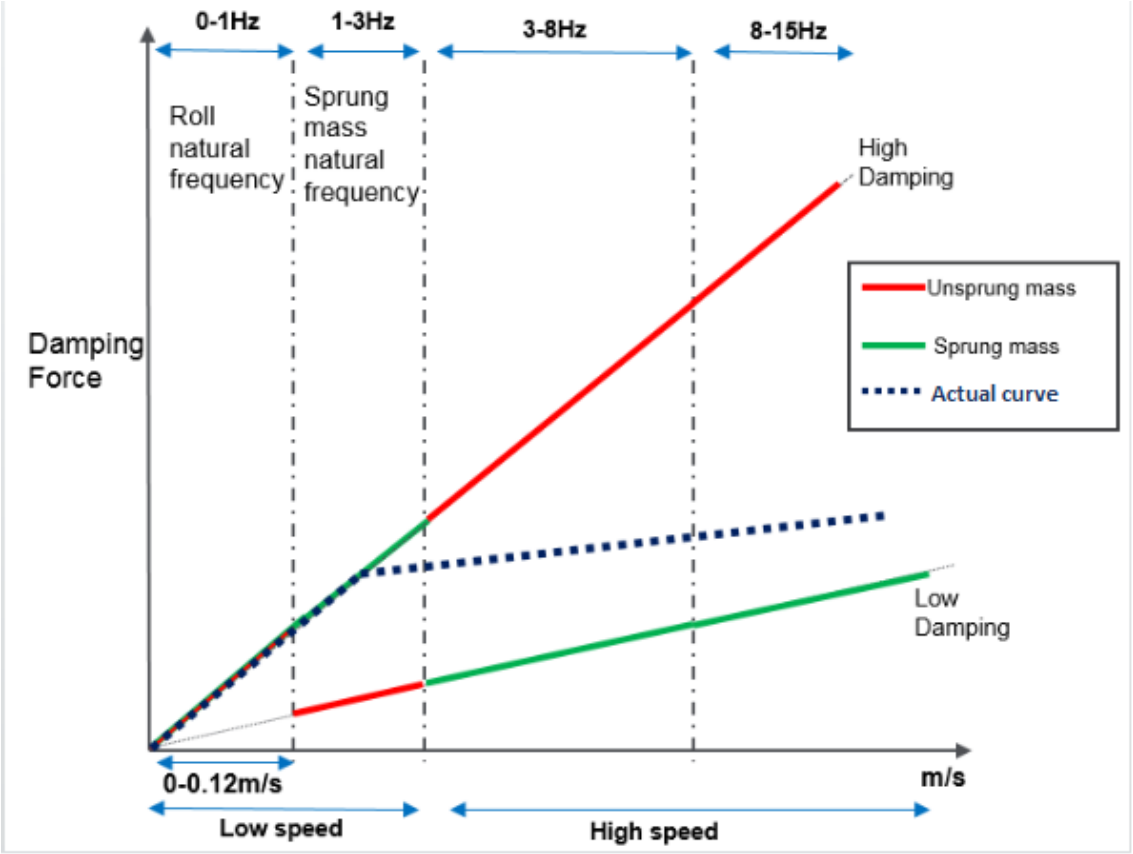

Figure 5.1: Depiction of F-v curve based on requirements

In the roll frequency region, the ideal situation would be to control the roll motion of sprung mass, hence high damping value should be chosen to control the transmissibility. Similarly, to control the sprung mass resonance, high damping value should be chosen around that frequency range as well but at the same time the unsprung mass damping should be low. In higher frequency region the idea should be to isolate the passengers cabin from road disturbances, so focus should be on reducing the acceleration of sprung mass, hence a lower value of damping should be chosen but for reducing the acceleration, unsprung mass requires a high damping value. Hence a compromise has to be done. It could be observed from Figure 5.1 that it is hard to meet the requirement for both sprung and unsprung masses using a passive system, hence a compromise has to be made based on the vehicle requirement. In the high velocity region the actual curve is between the sprung and unsprung mass requirement, the slope of which changes based on requirement. The high speed slope increase if focus is on unsprung mass behaviour, i.e better handling characteristic but this as a result will increase the sprung mass acceleration which will effect the isolation behaviour of sprung mass to make the ride uncomfortable. Tuning this is a tricky process as there is no optimized setting and it depends a lot on subjective feeling. Hence, this thesis helps in providing a detailed picture of the influence of damping force factors on sprung and unsprung masses rather than trying to provide an optimised damper setting for best performance.

6
Future Work

The findings from the work carried out in this thesis highlights the potential improvement in the development of dampers objectively. There are simplifications and limitations considered in this thesis, which forms the outline for future work in this regard. Some of the potential scope for future work is listed below.

- The difference between the different types of dampers to understand where they differ would be an interesting study. This can be achieved with having a common parameter across the different types of dampers, such as the linear range compression range and perform a frequency sweep analysis.

- **Development of the tool**
  The intention of the outcome of this thesis was to develop a tool which can present the results for changing damper specifications for any suspension setting. This could not be achieved within the time frame of the project, but the results certainly call for the development of a simple tool which can provide comparisons for changes in damper specifications for a desired system response

- **Frequency selective damping**
  Simulations with damping that changes with frequency (low/high) can be performed to investigate the variation/similarities of the influence of the identified metrics

- **Asymmetric Vehicle Model**
  The vehicle models considered for half-car simulations are symmetric in nature with same suspension parameters for each suspension. This can be extended to include individual suspension parameters and model an asymmetric vehicle with respect to dimensions

- **Advanced Half-car Model**
  In this thesis, the effect of roll motion is independently investigated but it will be interesting to see the coupled behaviour of roll and bounce motion together. Also complexity can be increased by adding the effect of anti roll bar and also

looking into the pitch behaviour.

Bibliography

[1] Fukushima, N., Hidaka, K. and Iwata, K. (1983) 'Optimum characteristics of automotive shock absorbers under driving conditions and road surfaces', *Int. J. of Vehicle Design*, vol. 4, no. 5, pp. 463-472.

[2] Sekulic D. et al., (2011) 'The Effect of Stiffness and Damping of the Suspension System Elements on the Optimisation of the Vibrational Behaviour of a Bus',*Int. J. of Traffic and Transport Engineering*,2011, 1(4): 231 – 244.

[3] Johnsrud, T. 'An Introduction to Dampers and the Black Art of Damper Tuning' www.theoryinpracticeengineering.com

[4] Giaraffa, M. and Brisson, S. Tech Tip: Spring & Dampers, Episode Four www.optimumg.com/docs/Springs&Dampers

[5] Pedro, M. et al., (1991) Vibration Mechanics, Kluwer Academic Publishers

[6] Jazar, R. N. (2008) Vehicle Dynamics Theory and Application. Springer

[7] Ihsan, S., Ahmadian, M. (2009) Ride Performance Analysis of Half-car Model for Semi-active System using RMS as Performance Criteria, Shocks & Vibrations,16 (6), 593-605.

[8] Mitra, A.C, Soni,T. (2015) Experimental Design and Optimization of Vehicle Suspension System. ScienceDirect,Materials Today: Proceedings 2 (2015) 2453 – 2462

[9] Dixon, J. C. (2008) The Shock Absorber Handbook, John Wiley & Sons

[10] Rajalingham C.,Rakheja s. / Influence of suspension damper asymmetry on vehicle vibration response to ground excitation, Journal of Sound and Vibration 266 (2003) 1117–1129

[11] Silveira M., et al. / Use of nonlinear asymmetrical shockabsorber to improve comfort on passenger vehicles, Journal of Sound and Vibration 333 (2014) 2114–2129

[12] Norman, K.N Controls system engineering. John Wiley & Sons

[13] Janschek, K. (2011) Mechatronics Systems Design. Springer

[14] Jacobson, B. et al., (2016) Vehicle Dynamics Compendium for course MMF062

A

Appendix 1

Table A.1: Parameters values of the 4-DoF half-car roll model

Parameter	**Description**
m	878.76 Kg
m_1	42.27 Kg
m_2	42.27 Kg
k_1	22589.2 N/m
k_2	22589.2 N/m
k_{t1}	200000 N/m
k_{t2}	200000 N/m
I_y	820 $Kg - m^2$
a_1	0.7 m
a_2	0.7 m